



## Review article

# A review of solid oxide cell technologies for power, fuel, and reversible energy storage

Bruna Rijo, Cecilia Mateos-Pedrero<sup>\*</sup>, José R. Copa Rey, Andrei Longo, Paulo Brito, Catarina Nobre

VALORIZA – Research Center for Endogenous Resource Valorization, Portalegre Polytechnic University, Campus Politécnico 10, 7300-555 Portalegre, Portugal



## ARTICLE INFO

## Keywords:

Electrolysis technologies  
Fuel cell technologies  
rSOC  
Renewable electricity renewable fuels

## ABSTRACT

Solid oxide cell (SOC) technologies, encompassing solid oxide fuel cells (SOFCs), solid oxide electrolysis cells (SOECs), and reversible solid oxide cells (rSOCs), are emerging as key components in the transition to sustainable energy systems due to their high operating efficiency, fuel flexibility, carbon-neutral fuel production potential, and compatibility with renewable energy sources. This work reviews current SOC technologies for renewable electricity generation and sustainable fuel production, examining their working principles and system configurations. Recent advances in materials, stack design, and control strategies are reviewed alongside significant challenges in material stability, dynamic response, electrode degradation, thermal management, and scalability. The paper highlights demonstration projects and provides an economic feasibility analysis of each SOC technology. Among electrolysis technologies, SOEC has higher capital expenditure (CAPEX) and operational expenditures (OPEX), but lower hydrogen production costs. A Strengths, Weaknesses, Opportunities, and Threats (SWOT) analysis reveals that SOEC possesses high hydrogen production efficiency, while SOFC offers great flexibility in fuel usage. However, it also points out that thermal stress and component degradation are significant challenges that need to be addressed. For rSOC, the analysis highlights the advantages of flexibility for two-way operation, along with concerns about stack cell degradation. The review also identifies innovation pathways needed to transition these systems from advanced prototypes to reliable components of decarbonised energy infrastructure, focusing on cost-effective materials development, electrode optimisation, and enhanced mathematical modelling.

## 1. Introduction

Solid oxide cells (SOCs) have emerged as a flexible platform for energy conversion, operating in three complementary designs: fuel-producing electrolyzers (SOECs), electricity-generating fuel cells (SOFCs), and reversible systems (rSOCs). These technologies leverage high-temperature electrochemistry (600–1000 °C) through ceramic electrolytes to achieve outstanding efficiencies (60–80 %) while maintaining fuel flexibility around hydrogen, methane, and ammonia. This operational versatility places SOCs as key enablers for decarbonised energy systems, capable of attending to both power generation and energy storage needs [1,2].

Recent material advances have transformed SOC capabilities. Using nanostructured electrodes with perovskite materials can lower polarisation losses by about 30 %. In addition, very thin electrolytes (less than 10 μm) allow the cells to work efficiently at lower temperatures

(650–750 °C) [3–5]. These developments support distinct applications for each configuration: SOFCs excel in distributed generation (85 % combined heat and power (CHP) efficiency), SOECs in power-to-X systems (> 70 % conversion efficiency, based on lower heating value (LHV)), and rSOCs in grid-balancing roles through bidirectional operation. Notably, proton-conducting electrolytes like  $\text{BaZr}_{0.8}\text{Y}_{0.2}\text{O}_{3-\delta}$  (BZY) have expanded SOEC capabilities for high-purity hydrogen production [6–11].

Field deployments demonstrate growing technological maturity. Industrial-scale SOFCs now achieve over 60 % electrical efficiency (defined here as the ratio of net electrical power output to the chemical energy input based on the fuel's LHV) in CHP applications, while SOEC systems successfully produce syngas for Fischer-Tropsch processes [12–15]. The GrInHy project validated rSOC operation at 150 kW scale, demonstrating 60 % round-trip efficiency, i.e., the ratio of electrical energy recovered in fuel-cell mode to the electrical energy consumed

<sup>\*</sup> Corresponding author.

E-mail address: [cecilia.pedrero@ippportalegre.pt](mailto:cecilia.pedrero@ippportalegre.pt) (C. Mateos-Pedrero).

<https://doi.org/10.1016/j.fuel.2025.137624>

Received 6 August 2025; Received in revised form 31 October 2025; Accepted 18 November 2025

Available online 27 November 2025

0016-2361/© 2025 The Author(s). Published by Elsevier Ltd. This is an open access article under the CC BY-NC-ND license (<http://creativecommons.org/licenses/by-nc-nd/4.0/>).

during electrolysis, with hydrogen production for steel annealing [16]. However, persistent challenges include degradation mechanisms (redox cycling, chromium poisoning) and high costs (~1000 \$/kW), though scalable manufacturing could reduce prices below 400 \$/kW by 2030 [17–21].

Despite substantial progress, the literature remains fragmented, with many studies focusing on isolated aspects such as material development, single-mode performance, or cost analysis, rather than providing an integrated assessment of how SOEC, SOFC, and rSOC technologies compare and complement each other [22–25]. Moreover, existing reviews often emphasise individual components or laboratory-scale studies without linking them to system-level integration, techno-economic viability, and industrial readiness [23,26]. This creates a clear research gap concerning the comprehensive evaluation of SOC technologies across their full value chain, from fundamental electrochemical mechanisms to large-scale demonstration and commercialisation pathways.

The present review addresses this gap by systematically analysing the current state of SOC development with emphasis on materials innovation, performance evolution, techno-economic indicators, and real-world demonstration projects. Furthermore, it positions itself by contrasting the strengths, weaknesses, opportunities, and threats (SWOT) of SOEC, SOFC, and rSOC systems, thereby clarifying their respective roles within emerging hydrogen, power generation, and energy storage markets.

Recent studies further emphasise the importance of integrating SOC technologies into decarbonisation strategies by combining techno-economic analysis with system-level modelling of renewable integration [27]. Complementary work highlights the need for improved durability, scalable stack manufacturing, and policy support to accelerate commercialisation [28], reinforcing the focus of this review on identifying innovation pathways for SOC deployment.

This review provides a thorough assessment of SOC technologies across their entire value chain, from fundamental operating principles to scaled-up demonstrations. The analysis begins with an overview of SOEC and SOFC systems, detailing their respective components, technological evolution, and economic considerations. This is followed by a discussion regarding rSOC systems, which addresses their unique configuration challenges and bidirectional operational requirements. The review then benchmarks real-world progress through an analysis of global demonstration projects across all three configurations. Finally, a SWOT analysis is presented that synthesises technological capabilities with market realities, offering actionable insights into future development pathways.

## 2. Solid oxide electrolyser cells (SOEC)

### 2.1. Working principles and components

An SOEC is an advanced electrochemical device that facilitates high-temperature electrolysis for the decomposition of steam into hydrogen and oxygen, or the conversion of carbon dioxide into carbon monoxide and oxygen, through the application of an external electrical current. Co-electrolysis of steam and carbon dioxide can also be performed in an SOEC [29]. In this process, a mixture of carbon monoxide and hydrogen, known as syngas, is produced directly. This mixture can then be transformed into a hydrocarbon fuel through additional methods, such as the Fischer–Tropsch process, methanol and ammonia synthesis, or the Sabatier process [30]. A schematic diagram of water-based SOEC technology is depicted in Fig. 1.

As shown in Fig. 1, an SOEC operates by conducting oxygen ions through a solid oxide or ceramic electrolyte at high temperatures, typically between 500 °C and 900 °C [31,32]. The high operating temperatures enhance reaction kinetics, reducing the electrical energy requirement when compared to conventional low-temperature electrolysis systems. This process leverages the thermal energy available at

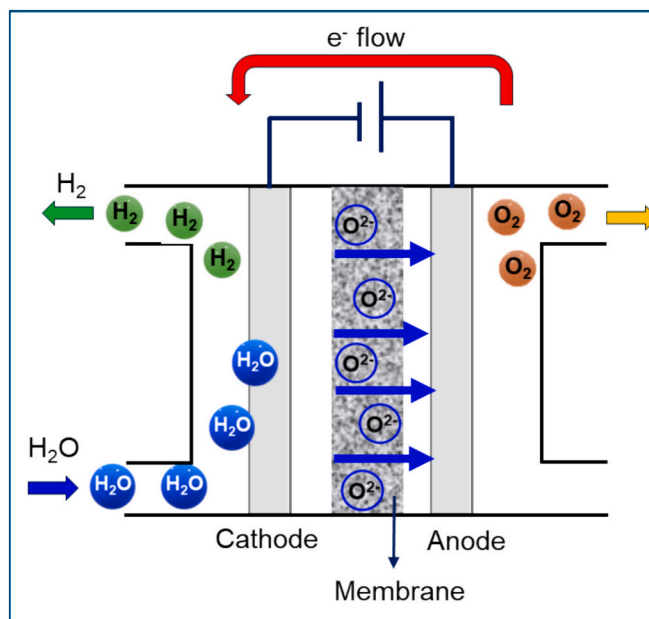


Fig. 1. Schematic diagram of water-based SOEC technology.

high temperatures and allows for the integration of external heat sources, thus improving overall efficiency. To provide a comprehensive overview of materials selection in solid oxide cell technologies, Table 1 summarizes representative anode, electrolyte, and cathode materials commonly used in SOECs, SOFCs, and rSOCs. Although this section primarily focuses on SOECs, highlighting their unique challenges and recent advances, the table includes comparative information for SOFC and rSOC configurations to underscore both the shared and distinct material choices across these related technologies. This context facilitates a clearer understanding of how advances in material development underpin the performance and operational stability of SOECs relative to other SOCs.

In terms of its structure, an SOEC comprises several key components that work together efficiently (Table 1) [33,34]. The electrolyte, a dense ceramic layer typically made from yttria-stabilised zirconia (YSZ), is known for its ability to conduct oxygen ions at high temperatures while serving as an insulator for electrons. The cathode, or negative electrode, is assembled from a porous material, often a nickel-YSZ cermet, where reduction reactions occur, enabling effective electricity conduction. On the other hand, the anode, or positive electrode, is typically constructed from perovskite materials such as lanthanum strontium manganite (LSM,  $\text{La}_{1-x}\text{Sr}_x\text{MnO}_{3-\delta}$ ) or lanthanum strontium cobalt ferrite (LSCF,  $\text{La}_{1-x}\text{Sr}_x\text{Co}_{1-y}\text{Fe}_y\text{O}_3$ ), which facilitates oxidation reactions during the cell's operation. A separator is also a critical component, electrically isolating individual cells within a stack to prevent short circuits while enabling ionic and thermal conduction between neighbouring cells. Solid electrolyte YSZ is frequently used for this purpose in SOECs. In addition, the gas diffusion layer (GDL) plays a crucial role in evenly distributing gases across the electrodes, ensuring the efficient delivery of reactants such as carbon dioxide and steam to the cathode and removing products such as carbon monoxide and hydrogen. Standard GDL materials are nickel mesh or foam, due to their high electrical conductivity, chemical compatibility with Ni-YSZ cathodes, and porous structure that allows efficient gas diffusion and mechanical robustness. Stainless steel meshes or porous sintered steels are often used in planar stacks or configurations where mechanical strength, and oxidation resistance are critical. To minimise corrosion, surface coatings such as  $\text{LaCrO}_3$  or  $\text{MnCo}_2\text{O}_4$  may be applied. Ceramic-based materials, including La-doped strontium titanate ( $\text{SrTiO}_3$ ) and perovskite oxides, also serve as good alternatives, but are less developed. These materials are favoured for their potential to

**Table 1**  
Summary of key functional materials in SOCs.

Cell type	Materials Anode	Electrolyte	Cathode	Ref.
SOFC	Ni–YSZ cermet; Ni–GDC (nickel/gadolinia–doped ceria); doped perovskites (e.g. LST, LSF, SFM, PBC)	YSZ; ScSZ; GDC; SDC; LSGM	LSM; LSCF (La <sub>1-x</sub> Sr <sub>x</sub> Co <sub>1-y</sub> Fe <sub>y</sub> O <sub>3</sub> ); BSCF; SFM; Ruddlesden–Popper; LSC	[26–29]
SOEC	Ni–YSZ; Ni–GDC; Ni–Cu–GDC; exsolved catalysts (e.g. Fe–Ni/GDC); doped perovskites for durability	YSZ; GDC; ScSZ; LSGM (same as SOFC)	LSCF; LSM; composites such as LSCF–GDC, LSM–SDC; high-performance layered cathodes (BSCF, double–perovskite structures)	[28,30–32]
rSOC	Ni–YSZ; Ni–GDC; redox-stable perovskites (LST, SFM, Sr <sub>2</sub> Fe <sub>1-5</sub> Mo <sub>0.5</sub> O <sub>6</sub> ); exsolved catalyst structures on GDC	YSZ; ScSZ; GDC; LSGM (emphasizing cycling stability)	LSCF; LSC; MIECs such as BSCF, SFM, LSCM; Ruddlesden–Popper and double perovskites optimized for reversible operation	[26,28,29]

improve long-term stability and reduce nickel coarsening [35–37].

Lastly, bipolar plates connect adjacent cells in series, managing gas flow through the system. These plates work as current collectors, gas distributors, and heat exchangers, and they are often made from cobalt-coated stainless steel to ensure durability and optimal stack performance. The electrochemical reactions in SOECs running steam electrolysis involve the steps detailed in Table 2 [38].

## 2.2. Technological evolution and current state of SOEC

Since 2015, SOEC technology has evolved from small-scale laboratory prototypes to increasingly robust and scalable systems.

Early developments were limited to capacities below 10 kW, mainly due to short lifespans, degradation during thermal cycling, and high costs associated with ceramic materials and stack manufacturing [39,40]. Nevertheless, research into advanced compositions of oxygen and hydrogen electrodes, improved interconnect coatings, and innovative stack designs gradually addressed these challenges.

By the early 2020 s, enhancements in thermal integration, current density (exceeding 1 A/cm<sup>2</sup>), and stack durability (targeting over 20,000 h) enabled reliable operation at multi-kilowatt scales. For example, Schwarze et al. [41] reported SOEC co-electrolysis operations with current densities above 0.5–0.65 A/cm<sup>2</sup>, achieving an efficiency of 85 % LHV and maintaining operation for over 4,100 h in pilot setups with approximately 150 kW systems. Subsequently, pilot systems with capacities of 250–400 kW and beyond were developed by companies like Sunfire and MHI (Mitsubishi Heavy Industries) [42].

These advancements have expanded the range of SOEC applications

**Table 2**

Key reactions and mechanisms in SOEC operation for steam, CO<sub>2</sub>, and co-electrolysis processes.

Location	Reaction	Comments
Cathode (steam reduction)	$2\text{H}_2\text{O}(\text{g}) + 4\text{e}^- \rightarrow 2\text{H}_2(\text{g}) + 2\text{O}^{2-}$	Steam molecules are reduced to hydrogen gas and oxide ions by gaining electrons. The oxide ions then move through the solid electrolyte from the cathode to the anode.
Anode (oxidation)	$2\text{O}^{2-} \rightarrow \text{O}_2(\text{g}) + 4\text{e}^-$	The oxide ions release electrons and form oxygen gas.
Overall (steam electrolysis)	$2\text{H}_2\text{O}(\text{g}) \rightarrow 2\text{H}_2(\text{g}) + \text{O}_2(\text{g})$	—
Cathode (CO <sub>2</sub> reduction)	$\text{CO}_2(\text{g}) + 2\text{e}^- \rightarrow \text{CO}(\text{g}) + \text{O}^{2-}$	Carbon dioxide gains electrons to form carbon monoxide and oxide ions. The anode reaction is the same as in steam electrolysis.
Overall (CO <sub>2</sub> electrolysis)	$\text{CO}_2(\text{g}) \rightarrow \text{CO}(\text{g}) + \frac{1}{2} \text{O}_2(\text{g})$	—
Cathode (co-electrolysis)	$2\text{H}_2\text{O}(\text{g}) + 4\text{e}^- \rightarrow 2\text{H}_2(\text{g}) + 2\text{O}^{2-}$ $2\text{CO}_2(\text{g}) + 4\text{e}^- \rightarrow 2\text{CO}(\text{g}) + 2\text{O}^{2-}$ $\text{CO}_2(\text{g}) + \text{H}_2(\text{g}) \rightarrow \text{CO}(\text{g}) + \text{H}_2\text{O}(\text{g})$	In co-electrolysis, both H <sub>2</sub> O and CO <sub>2</sub> are reduced simultaneously at the cathode. The reverse water–gas shift reaction occurs concurrently [23,39].

beyond hydrogen production, including co-electrolysis for syngas, synthetic methane, methanol, and ammonia, particularly within industrial sectors that need to integrate high-temperature waste heat [41]. While challenges (e.g., cost, lifespan, and system standardisation) remain, SOECs are increasingly recognised as high-efficiency platforms for carbon–neutral fuel production and large-scale industrial decarbonisation [43,44].

By 2025, automated pilot production lines, such as the ThyssenKrupp Nucera–Fraunhofer IKTS facility in Arnstadt, Germany, are expected to produce SOEC stacks at 8 MW per year, thereby accelerating their commercial readiness [45]. The Arnstadt facility utilises planar stack configurations that incorporate nickel-YSZ fuel electrodes alongside LSCF oxygen electrodes, operating at approximately 800 °C. The production line is designed to achieve stack lifetimes exceeding 20,000 h and current densities of over 0.8 A/cm<sup>2</sup>. To ensure both reliability and scalability, the facility incorporates integrated thermal management and automated quality control systems, which help maintain consistent production standards.

In parallel, Elcogen began installing the world’s largest SOEC unit at a steel plant in March 2025, focusing on hydrogen and syngas production through co-electrolysis [46,47]. The Elcogen unit comprises over 1,000 solid oxide electrolysis cells organised into modular stacks. Each stack operates at temperatures ranging from 700 to 750 °C, delivering a system-level current density of approximately 0.6 A/cm<sup>2</sup>. Designed for flexibility, the co-electrolysis process enables the production of syngas with H<sub>2</sub>/CO ratios adjustable between 1.5 and 2.2, allowing for various downstream synthesis routes. Advanced features such as real-time degradation monitoring and adaptive control systems ensure optimal operation under dynamic industrial loads.

Systems are now routinely operating at 250–600 kW capacities, producing hydrogen at approximately 37 kWh/kg, with an efficiency of about 65–70 % LHV, and ongoing performance improvements [42,48]. Recent pilot demonstrations have achieved Faradaic efficiencies exceeding 95 %, alongside area-specific resistances of below 0.5 Ω·cm<sup>2</sup>, providing clear evidence of significant advances in both stack engineering and interconnect development. Typically, these systems operate at pressures of up to 5 bar, allowing for seamless integration with downstream synthesis reactors without the necessity for intermediate compression.

A key advantage of SOECs is their ability to perform co-electrolysis, producing a customisable syngas that can be utilised for downstream synthesis of hydrocarbons. For instance, the North-C-Methanol project in Belgium, launched in 2023, aims to produce 44,000 t of green methanol annually using hydrogen from electrolysis and captured industrial CO<sub>2</sub> [49]. The North-C-Methanol project incorporates SOEC stacks with operating temperatures of 750–800 °C and current densities of 0.5–0.7 A/cm<sup>2</sup>. The system is integrated with a methanol synthesis loop that uses a Cu/ZnO/Al<sub>2</sub>O<sub>3</sub> catalyst, optimised for syngas compositions generated via co-electrolysis. The overall process targets a conversion efficiency of 60–65 % and includes heat recovery units to improve exergy performance.

Similarly, SOEC-based fuel synthesis pathways are gaining attention in ammonia production, as seen in the GAPP pilot in Morocco and the

Skipavika Green Ammonia project in Norway, which targets over 100,000 t/y by 2027 [50,51]. Both the GAPP and Skipavika projects utilise SOEC modules operating at 700–750 °C, with stack capacities ranging from 500 to 1,000 kW. The systems are designed for integration with ammonia synthesis loops based on Haber–Bosch reactors and include dynamic load-following capabilities to accommodate fluctuations in renewable energy.

In the coming years, SOEC systems will be pivotal in decarbonising industries, especially in sectors that can access high-temperature waste heat and CO<sub>2</sub> streams. Anticipated trends include the development of modular multi-megawatt installations, the integration of renewable energy-powered heat sources, and hybrid systems that combine SOECs with downstream synthesis reactors. Furthermore, digital control strategies and predictive maintenance advances are expected to extend stack lifetimes and reduce operational costs. As manufacturing scales up and supportive policy measures take effect, SOEC deployment could expand into the steel, cement, and chemical sectors, contributing significantly to net-zero targets across Europe and beyond.

To ensure a consistent assessment of technological progress, Fig. 2 summarises the evolution of SOEC performance using a unified set of indicators commonly adopted in the literature: (i) current density at 1.3 V and 700–800 °C, (ii) electrical-to-hydrogen conversion efficiency, and (iii) voltage degradation rate (mV/kh). Based on these metrics, SOEC technology has advanced from early high-temperature systems (< 0.5 A/cm<sup>2</sup> at 850 °C, ≈ 65 % efficiency, > 40 mV/kh degradation) to modern intermediate-temperature configurations exceeding 1.5 A/cm<sup>2</sup>

at 700 °C with efficiencies of 80–85 % and degradation rates below 10 mV/kh. This unified framework highlights the continuous improvement in materials and stack engineering that underpins the transition from laboratory-scale cells to commercially relevant systems.

### 2.3. Hydrogen production via SOEC systems

Hydrogen is the most widely studied product in SOEC research due to its central role in clean energy systems and high energy density. Even though hydrogen can be produced through other water electrolysis technologies, such as alkaline water electrolyzers (AWE) and proton exchange membrane (PEM) electrolyzers, SOEC offers unique advantages in terms of efficiency and integration with high-temperature processes. This section focuses on hydrogen generation via SOEC, laying the groundwork before exploring additional electrolysis products in subsequent sections.

Nasser et al. [52] investigated hydrogen production from waste heat using two different electrolyser systems: PEM and SOEC. In their setup, a Rankine cycle converts the energy from exhaust gases into electricity, which powers the electrolysis process. Additionally, part of the exhaust gas is used to preheat the water feed. Under all evaluated waste heat input conditions, the SOEC system consistently outperformed the PEM system in both hydrogen output and overall efficiency. At an operating temperature of 780 °C, SOEC achieved a hydrogen production rate of 36.9 kg/h with a system efficiency of 23.8 %, defined as the ratio of the useful energy contained in the produced hydrogen to the input waste heat energy, consistent with the approach adopted by Nasser et al. In contrast, the PEM system reached 27.4 kg/h at an efficiency of only 14.5 %. This comparison highlights SOEC's superior performance in thermally integrated setups, especially when waste heat is available.

Recent literature has critically examined the main electrolysis technologies for hydrogen production, emphasising emerging developments and persistent challenges. For example, El-Shafie [53] compares the main water technologies for hydrogen generation, PEM, AWE, anion exchange membrane (AEM), and SOEC. Among these, PEM exhibits a superior ability to produce high-purity hydrogen with ease of handling and maintenance, but its cost remains high. On the other hand, AEM technology benefits from lower hydrogen production costs compared to PEM and AWE, utilising cost-efficient transition metal electrocatalysts, such as Ni, Fe, or Mo, rather than the noble metal catalysts employed in the latter technologies. Nevertheless, AEM performance requires significant improvement to be competitive in large-scale hydrogen production. The main challenges of AWE technology are primarily associated with fluctuations in input power and catalytic degradation over time. In contrast, SOEC technology boasts high conversion efficiency, low operating costs, and reduced emissions, but its high-temperature operation leads to longer startup times. Despite this, SOECs are well-suited for integration into high-temperature industrial processes. Considering all the studies, PEM and AEM provide benefits in terms of purity and cost. In contrast, SOEC stands out as the most promising method for large-scale, thermally integrated hydrogen production.

The review by Zainal et al. [54] provides an assessment of the primary hydrogen production electrolysis methods, focusing on their cost-effectiveness, environmental impact, and level of technological development. According to the authors, the SOEC currently outperforms other electrolyser types, with AEM also showing promise. AWEs are a mature technology for producing high-purity hydrogen on a large scale. AEM and PEM electrolyzers can be more efficient and cost-effective than traditional AWE options, with faster response times. SOECs, while the most efficient, remain the most expensive and are still under development. Their high-temperature operation can be integrated with industrial processes and use waste heat. SOECs also have a higher electrochemical reaction rate and lower energy requirements, and they can operate in co-electrolysis mode to produce syngas from steam and carbon dioxide. This reinforces the earlier findings and positions SOEC

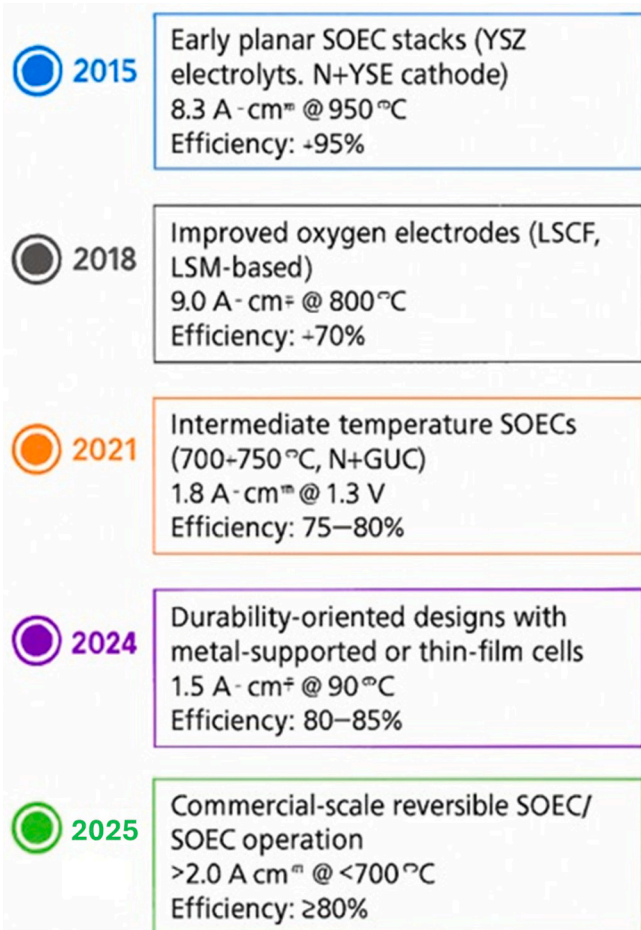


Fig. 2. Evolution of SOEC technology from 2015 to 2025, based on representative literature data. Each milestone indicates progress in stack architecture, electrode and electrolyte materials, and operational performance under unified reference conditions.

as a high-efficiency option for sectors where heat recovery and CO<sub>2</sub> utilisation are feasible.

Wang et al. [31] provide a systematic analysis of advanced operation scheduling strategies for AWE, PEM, and SOEC. The most relevant operational characteristics of these technologies are compared in Table 3.

The authors concluded that AWE is the most widespread electrolysis technology primarily due to its high commercial maturity, lower cost, high tolerance to impurities, and long lifetime. Despite PEM systems offering dynamic response capabilities and a more flexible load range, which makes them suitable for renewable energy systems, their high cost associated with the use of Pt-group catalysts and expensive membrane production prevents their broader expansion. On the other hand, high-temperature SOEC technology remains at a lower level of industrialisation. Nonetheless, it rapidly approaches commercialisation and shows strong potential, especially in applications prioritising high efficiency and continuous operation. This comparative analysis confirms that SOEC's niche lies in steady-state, high-throughput industrial contexts, rather than intermittent renewable-driven setups.

The review by Nnabuife et al. [55] analyses recent progress in AWE, PEM, and SOEC technologies, alongside emerging strategies for grid integration and energy storage, to support the deployment of green hydrogen. Despite significant advances in coupling renewables with electrolysis for green hydrogen, key areas still require additional research and development. These areas include improving electrolyser efficiency and durability through advanced materials and catalyst design, developing smart grid integration strategies for renewable-based hydrogen, exploring cutting-edge energy storage solutions, and assessing the full environmental impact of green hydrogen systems. This broader systems-level view complements the technology-specific comparisons above, underscoring the importance of integrating SOECs into smart, decarbonised energy infrastructures.

In line with the reports above, Akyüz et al. [56] highlight the importance of water electrolysis technologies in the transition toward a cleaner energy system. The authors explain that different types of electrolysers each have their advantages and disadvantages. For instance, AWE systems are effective but struggle with varying energy sources. PEM electrolysers are efficient, yet they require costly materials. In contrast, AEM electrolysers combine the advantages of both AWE and PEM systems while being more affordable. SOECs are recognised for their efficiency, but they operate at high temperatures. Ultimately, the authors note that the best choice of electrolyser depends on

**Table 3**  
Comparison of technical characteristics of AWE, PEM, AEM, and SOEC technologies [24].

Parameter	Electrolysis technology			
	AWE	PEM	AEM	SOEC
Start-up time	Moderate Warm start-up 1–5 min Cold start-up 30–60 min	The quickest Warm start-up ~10 s Cold start-up 5–10 min	Intermediate Warm start-up: 1–2 min Cold start-up: 10–30 min	The slowest Warm start-up ~15 min Cold start-up 6–10 h
Shutdown time	Moderate (a few mins)	The quickest (a few seconds)	Moderate (1–5 min);	The slowest (up to 10 mins)
Load range	Acceptable load flexibility (15 %–100 %)	Exceptional load flexibility (5 %–120 %)	High load flexibility (10 %–100 %)	Exceptional load flexibility (30 %–125 %)
Ramp rate	Moderate (0.17 %–0.33 %/s)	High (>10 %/s)	Moderate–High (~1–5 %/s)	Slow (~0.083 %/s)

the specific application, available resources, infrastructure, and economic feasibility. This synthesis confirms that SOECs are best suited for stable, high-temperature industrial environments, while PEM and AEM may be more adaptable to variable renewable inputs.

Liu et al. [29] offer a timely overview of recent advancements in SOEC technology, spanning from cell-level innovations to stack and system integration. Over the past decade, SOEC technology has progressed significantly from laboratory research to commercial viability, thanks to advancements in materials, design, and manufacturing. Notable improvements in components such as cell interconnects and sealants have decreased area-specific resistance and contributed to longer operational lifespans across various SOEC designs. Many degradation mechanisms have been thoroughly analysed, and practical strategies to mitigate these issues have been successfully implemented. Nevertheless, key challenges such as efficiency, durability, and cost persist. Addressing them is essential for establishing SOEC as a leading electrochemical energy solution. The authors emphasise that for commercial viability, SOECs must lower hydrogen production costs by extending lifespan under milder conditions and higher currents, cutting capital expenses through cost-effective materials and scalable manufacturing, and enabling business models through flexible operation and value-chain integration. Liu et al.'s review offers a significant overview of the progress made in SOEC, shedding light on innovations at both the cell level and in system integration. Based on their insights, we stress that future advancements should focus on developing cost-effective materials, scalable manufacturing processes, and adaptable operational strategies. These factors are crucial for unlocking the full potential of SOEC in the pursuit of industrial decarbonisation.

The existing literature highlights that AWE and PEM technologies are currently well-suited for deployment due to their established reliability and responsiveness.

Otherwise, SOEC is recognised as a promising alternative due to its high efficiency and great potential for integration in high-temperature industrial processes. Through effective use of waste heat and sustained high-efficiency operation, SOEC technology holds strong potential to support the decarbonisation of energy-intensive industrial sectors.

#### 2.4. SOECs-enabled methanol synthesis

SOECs facilitate the simultaneous electrochemical conversion of multiple feedstocks, such as carbon dioxide and water, within a single, integrated process known as co-electrolysis, in contrast to conventional water electrolysis, which produces only hydrogen. For instance, syngas from carbon dioxide and water co-electrolysis is a valuable intermediate in generating many products of interest, like methanol, a critical chemical feedstock and energy vector. As such, SOEC-based co-electrolysis stands out as a promising technology in advancing sustainable chemical manufacturing and enabling circular carbon utilisation.

One illustrative example of this potential is the work by Syauqi et al. [57], who investigated the use of SOEC for co-electrolysing carbon dioxide and water from steel industry emissions to produce syngas for methanol synthesis. They developed a deep neural network-based surrogate model that accurately predicted outputs. Optimising conditions (high temperature, low current density, reduced steam flow) led to nearly tenfold methanol productivity compared to systems without SOEC. This integration also drastically reduced the plant's carbon footprint, projecting near-zero carbon dioxide emissions due to improved efficiency. This study demonstrates the dual benefit of SOECs in boosting methanol yield and reducing emissions when integrated with industrial waste streams.

The study by Fogel et al. [58] introduces a real-time model of a power-to-methanol system using proton-conducting high-temperature electrolysers (H-SOEC). Depending on the process design and heat integration, H-SOEC systems demonstrated efficiencies (in terms of LHV) between 0.488 and 0.637. Although the baseline efficiency (0.488) is lower than that of conventional oxygen-anion-conducting membrane

(O-SOEC) systems (up to 0.760), improvements such as better heat integration and higher flash separator pressure could increase it to 0.637. Reducing power consumption remains crucial for improving efficiency and lowering the costs of renewable methanol production. Compared to Syauqi et al., this study highlights the importance of system-level optimisation and membrane selection in achieving competitive efficiency.

Also aiming to produce renewable methanol from syngas generated by SOEC technology, Banu et al. [59] developed a system that uses several green technologies to produce clean energy efficiently. This system processes methane through thermal cracking to create hydrogen and carbon black. These products are used in PEM fuel cells (PEMFC) and direct current fuel cells (DCFC) to generate electricity. Meanwhile, a solar-powered SOEC system uses electricity generated from solar energy to drive the high-temperature electrolysis of water and carbon dioxide. This process produces syngas, which can be further processed into methanol. Using renewable solar power, the SOEC efficiently converts waste carbon dioxide and water into valuable chemical fuels, closing the carbon loop and reducing greenhouse gas emissions. This approach produces multiple clean energy products while capturing carbon as a solid, boosting overall efficiency and reducing emissions compared to standard SOEC hydrogen production. Overall, the system generates 7.71 MW of power, achieving an energy efficiency of 40.6 % and an energy efficiency of 37.5 %. This multi-stream integration contrasts with the previous studies by incorporating solar energy and carbon capture, showcasing SOEC's versatility in hybrid systems.

A similar concept of employing renewable sources to produce low-carbon methanol is investigated by Ostadi et al. [60]. In this study, the authors compare three routes to improve flexibility and increase methanol yield. First, the conventional biomass-to-methanol pathway, which relies on the use of biomass/municipal solid waste (MSW), natural gas (NG), and renewable power is studied. Additionally, hydrogen-enriched processes have been investigated, with hydrogen obtained through NG pyrolysis, steam electrolysis in an SOEC, or a combination of both methods. Adding external hydrogen significantly enhanced methanol production, increasing it from 44 % to 94 % for biomass and Mixed Ionic-Electronic Conductor (MIEC) compared to the conventional process. This process illustrates the benefits of diversifying feedstock to enhance the economic viability of the process by using the most cost-effective and available resources. In contrast to the solar-powered system proposed by Banu et al., this approach underscores the importance of feedstock diversity and external hydrogen input in enhancing methanol yields.

An interesting method for integrating biomass with the SOEC process to produce methanol is discussed by Detchusananard et al. [61]. Integrating biomass gasification with an SOEC enhances methanol production by improving syngas quality and system efficiency. Key factors influencing this process include the number of SOEC cells and their operating temperature, which are optimally set at 325 cells and 700 °C, thereby increasing hydrogen and oxygen output. The hydrogen adjusts the syngas composition for better carbon conversion, while the oxygen supports more efficient gasification without external air separation. Additionally, effective heat recovery from the high-temperature SOEC process reduces energy input. This integrated approach achieves a higher methanol yield (0.4995 kmol/h) and an overall efficiency of 64.8 %, surpassing conventional biomass-to-methanol methods in both performance and energy use. This study complements Ostadi et al. by showing how SOECs can enhance biomass conversion efficiency through targeted thermal and gas integration.

Recent research by Emadi et al. [62] has reported on an integrated system that combines direct air capture (DAC) of carbon dioxide with SOECs to produce methanol and syngas. The energy consumption, resource utilisation, and economic viability of these processes were analysed using Aspen Plus software. Assuming a DAC capacity of 250,000 t CO<sub>2</sub>/y, the production rates are 36.4 t/h of methanol or 15.1 t/h of syngas. Methanol production requires a specific energy

consumption of 26.0 kWh/kg. In comparison, syngas production has a higher energy requirement of 53.9 kWh/kg, resulting in lower carbon dioxide emissions per unit of product. By integrating direct air capture with SOECs, the approach introduces a carbon-negative pathway that enhances the sustainability profile of methanol synthesis.

In the same context, Park et al. [63] proposed an integrated bio-methanol process that combines the partial oxidation of biogas with the production of green hydrogen using a renewable-powered SOEC. The oxygen produced by the SOEC is reused for the oxidation of biogas, while the waste heat generated aids in steam production. This process feeds syngas and green hydrogen into the methanol synthesis unit, yielding 88.51 %. Additionally, this method improves energy efficiency by 177 % compared to conventional e-methanol processes and 7 % over traditional bio-methanol routes. In relation to Emadi et al.'s DAC-based configuration, this method prioritises resource circularity and thermal integration, highlighting a complementary pathway for SOEC deployment.

To promote sustainable methanol production using SOEC technology, the study by Abousalmia et al. [64] simulates and evaluates an integrated system that combines liquefied natural gas (LNG), the Allam–Fetvedt cycle, SOEC, and methanol synthesis. The Allam–Fetvedt cycle operates at 55 % efficiency, capturing 96 % of carbon dioxide for internal reuse. Co-electrolysis of the remaining 4 % carbon dioxide with steam produces syngas, which is fed into the methanol synthesis unit. Results show that this process supports large-scale production, yielding 1.38 × 10<sup>6</sup> t of methanol and 3.6 × 10<sup>6</sup> t of LNG annually. Despite the energy-intensive nature of electrolysis, efficient heat recovery and integration help maintain the system's overall energy performance. These results emphasise the potential of SOEC as a crucial facilitator for the efficient and low-carbon production of methanol. This large-scale scenario builds on previous pilot studies, demonstrating how SOECs can be integrated into high-throughput, carbon-capturing industrial ecosystems.

Taken together, recent studies demonstrate the versatility of SOEC-based co-electrolysis in enabling low-carbon methanol synthesis across diverse configurations—from solar-driven systems to biomass and DAC integration. In our view, the most impactful future developments will combine SOEC's high efficiency with circular carbon strategies and modular deployment. However, techno-economic optimisation and lifecycle assessment remain essential for guiding scale-up and ensuring environmental credibility.

## 2.5. Techno-economic aspects of SOEC technology

### 2.5.1. Comparative assessment of electrolysis technologies

Table 4 presents a comparison of the four main water electrolysis technologies (AWE, PEM, SOEC, and AEM), highlighting significant distinctions in terms of Technological Readiness Level (TRL), cost structures, and energy efficiency.

To complement the techno-economic comparison presented in Table 4, Fig. 3 provides a graphical summary of the capital expenditure (CAPEX) and levelised cost of hydrogen (LCOH) across the four main electrolysis technologies. The bar charts highlight the relative maturity of AWE and PEM systems, which currently offer lower CAPEX ranges, compared to SOEC technology, which exhibits higher initial costs but has the potential for significantly lower hydrogen production costs under favourable integration scenarios [64–68]. This visual representation makes the trade-offs between technologies more intuitive, while the detailed values remain available in the table for reference.

The comparative assessment of electrolysis technologies reveals a nuanced landscape where maturity, cost, and performance intersect with competing advantages. While AWE and PEM currently lead in commercial deployment due to their high TRL (8–9) and established supply chains, this maturity comes with inherent limitations. AWE's cost advantage (500–1,400 €/kW) and operational simplicity are counterbalanced by its low current densities and poor dynamic response,

**Table 4**  
Economic comparison of AWE, PEM, SOEC and AEM [54,65–67].

Technology	AWE	PEM	AEM	SOEC
TRL	9	8–9	6	6–8
Capital expenditures (CAPEX) (€/kW)	500–1,400	1,100–1,800	~1,000–1,500 (lab/pilot scale)	2,800–5,600
Potential to use earth-abundant and affordable materials	Limited (Ni, Co)	Limited (Pt-group metals, Ti)	High (transition metals, non-PGM catalysts, polymeric membranes)	Moderate (ceramics, Ni-YSZ, some critical oxides)
Operational Expenditure (OPEX), (% investment cost/year)	2–3	3–5	~2–4 (est.)	3–6 (stack lifetime dependent)
Stack capital cost (€/kWh) minimum 1 MWh	233	342	~400–600 (prototypes, projected)	>1712
Stack capital cost (€/kWh) minimum 10 MWh	428–856	599–1,198	300–600 (projected, GW-scale)	200–400 (projected, pilot-to-demonstration scaling).
Production cost (€/kgH <sub>2</sub> )	5.1	3.1–4.7	~4–6 (pilot studies, depending on membrane lifetime)	1.9–3.2
Average stack/system lifetime (h)	60,000–90,000	20,000–60,000	20,000–40,000 (target > 60,000)	2,000–10,000 (early prototypes)
Overall efficiency (LHV, %)	60–70	55–65	80–90 (with thermal integration)	60–70 (projected)

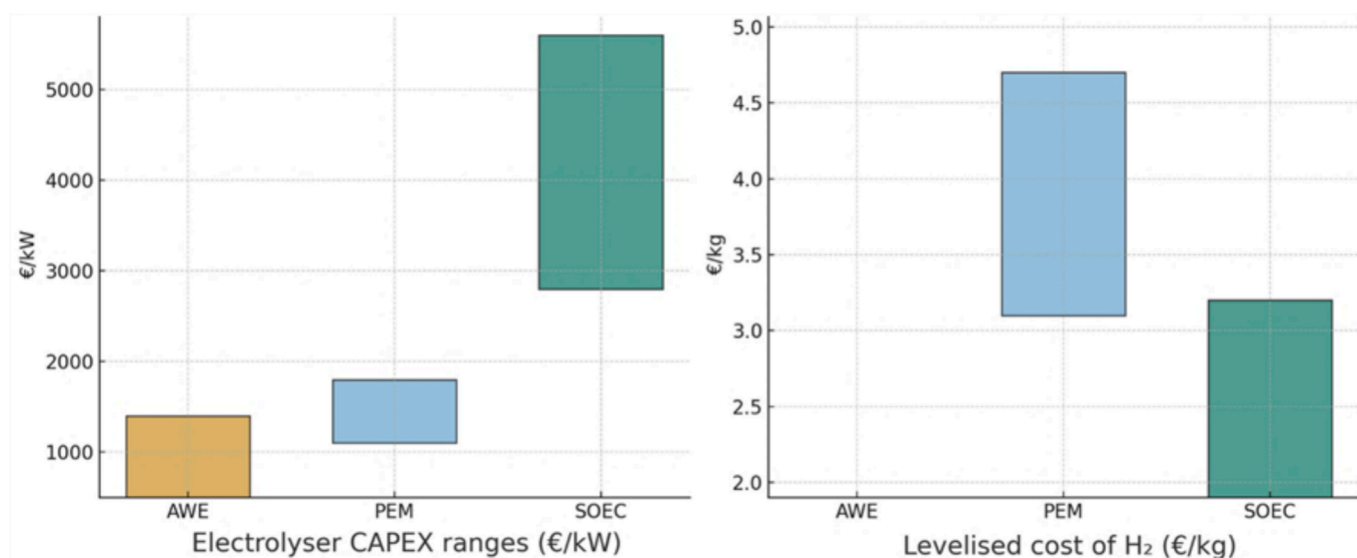


**Fig. 3.** Comparative techno-economic ranges of water electrolysis technologies (CAPEX and LCOH).

making it less suitable for renewable integration compared to PEM systems. PEM's faster load-following capability comes at a premium price of 1,100 to 1,800 €/kW, driven by the high cost of components such as platinum catalysts and titanium bipolar plates. However, ongoing research into alternative materials could reduce these costs by 30 % within this decade. The higher TRL technologies also face sustainability concerns, as both rely on critical materials that may limit their scalability. AWE's nickel anodes and PEM's platinum-group metals present supply chain risks as hydrogen demand grows.

Emerging technologies present different value propositions. SOEC's remarkable efficiency (> 85 % LHV) and ability to utilise waste heat or co-electrolyse carbon dioxide position it as a future cornerstone for industrial decarbonization, though its current TRL (6–8) reflects significant material challenges. The significant capital costs associated with this technology, which range from approximately €2,800 to €5,600 per kW<sub>e</sub>, alongside stack expenses between €350 and €800 per kW<sub>e</sub>, stem from the complex manufacturing processes and material requirements involved. Additionally, there are ongoing durability challenges, particularly the degradation of nickel and yttria-stabilised zirconia (Ni-YSZ) electrodes during thermal cycling. Recent techno-economic evaluations indicate the current costs for solid oxide electrolyser cell (SOEC) systems are around €4,000 to €5,000 per kW<sub>e</sub> in pilot-scale installations. However, projections suggest that stack-only costs could dramatically drop from about €370 per kW<sub>e</sub> in 2020 to below €50 per kW<sub>e</sub> by 2030 as

manufacturing scales up. Paradoxically, SOEC technology presents the lowest hydrogen production costs, estimated between €1.90 and €3.20 per kg of H<sub>2</sub>, under optimal, thermally integrated conditions. This highlights that its economic potential could improve significantly with greater integration of renewable energy sources and large-scale deployment.

AEM represents a different paradigm altogether – its theoretical ability to combine AWE's material simplicity with PEM's performance characteristics makes it potentially disruptive, though its TRL (6) indicates that fundamental challenges in membrane stability and catalyst durability must first be addressed. Early-stage research shows promise in replacing precious metals with transition-metal catalysts, but commercial viability remains unproven.

The economic analysis underscores how technology choices depend on operational context and time horizon. For near-term, small-scale applications, AWE's low CAPEX and proven reliability make it attractive despite higher production costs (5.10 €/kg). Medium-term scenarios favouring renewable integration may shift preference toward PEM, despite its higher maintenance costs (3–5 % of CAPEX/y), due to better dynamic response. The long-term outlook favours SOEC for large-scale, heat-integrated applications and AEM for distributed systems if material challenges are overcome. This technological bifurcation suggests that future hydrogen infrastructure may employ hybrid systems, combining mature technologies to meet immediate needs while developing

advanced electrolyzers to address future requirements. Critical to all pathways is addressing material bottlenecks, whether through SOEC's ceramic engineering, AEM's novel membranes, or PEM's catalyst optimisation, to achieve both economic viability and sustainability at scale.

### 2.5.2. Cost and performance considerations of SOEC systems

While all electrolyzers face cost sensitivity to electricity prices, SOECs' unique ability to leverage waste heat and co-electrolyse carbon dioxide positions them as a potentially cost-competitive pathway to synthetic fuels, if durability and scaling challenges are resolved. Lee et al. [65] proposed a decentralised approach integrating an SOEC with a small modular reactor (SMR). They analysed various configurations, factoring in carbon emission costs. With a 300 MW SOEC stack, they found that Case 1 achieved the lowest hydrogen production cost at 4.3 €/kg of hydrogen and the lowest carbon dioxide emissions at 0.36 kg/kg of hydrogen. The integrated SOEC/SMR configuration in the most favourable scenario (Case 1) outperforms, in terms of economic viability, more mature electrolysis technologies such as PEM and AWE systems powered with a mix of grid electricity and renewable electricity (7.3 and 5.8 €/kg H<sub>2</sub> for PEM and AWE, respectively) or fully renewable electricity (4.5–54.4 and 6.9–42.9 €/kg H<sub>2</sub> for PEM and AWE, respectively). These results demonstrate that this integrated strategy is a practical way to produce low-carbon hydrogen.

Fei et al. [66] carried out a techno-economic analysis (TEA) of a hydrogen production system based on the combination of an SOEC with a gasifier and a hydrogen separation membrane. A multi-objective optimisation was conducted to reduce the LCOH and the levelized carbon dioxide emissions (LCE). In this context, LCOH refers to the average cost of producing one unit (e.g., kilogram) of hydrogen over the entire lifespan of a production facility. In contrast, the LCE measures the average cost associated with emitting one unit of greenhouse gas throughout the lifetime of an energy system. Considering different payback periods, the corresponding hydrogen sales price was established under optimal conditions. Optimisation results indicate a minimum LCOH of 3.11 €/kg, corresponding to LCE of 10.17 kg CO<sub>2</sub>/kg H<sub>2</sub>. The system can accommodate emissions as low as 2.92 kg CO<sub>2</sub>/kg H<sub>2</sub>, resulting in an LCOH of 5.52 €.

The work conducted by Bui et al. [69] demonstrated the enhanced cost efficiency of a high-power SOEC system (2 MW), reducing hydrogen production costs by up to 23 % compared to a low-power SOEC system (20 kW). The stack cost was identified as the primary contributor to CAPEX, while the electricity cost emerged as the most significant factor influencing the overall hydrogen production cost. In the base case scenario, the hydrogen production cost is 6.60 €/kg for the high-power system, whereas it reaches 8.54 €/kg for the low-power counterpart.

As reported by Cavalcanti et al. [70], the TEA provides insights into an SOEC system powered by solar energy, which utilises a heliostat, photovoltaic panels, and a battery bank. This system operates at 950 °C and a current density of 2500 A/m<sup>2</sup>, enabling the 60-module setup to generate 112.8 kg/h of green H<sub>2</sub> while achieving an overall efficiency of 95.33 %. The photovoltaic panels and battery system boast an average efficiency of 18.02 %, while the solar field operates with an average efficiency of 34.6 %. In terms of costs, the solar field and the photovoltaic/battery system account for 42.52 % and 39.65 % of the total system expenses, respectively. The calculated LCOH stands at 8.1 €/kg.

In a recent study, Jiménez-Martín et al. [71] assessed the LCOH for an MW-scale SOEC system. Initial estimates exceed 6 €/kg, driven by electricity and stack costs, though optimistic scenarios suggest values below 4 €/kg. The authors point out that integration with heat-intensive industries such as cement or steel could further reduce costs.

Zhang et al. [72] developed a power-to-methanol system utilising SOEC co-electrolysis, achieving 72 % energy efficiency and 93.6 % carbon conversion. Nevertheless, production costs remain high at 458.6 €/t, with a payback period exceeding 11 years. The system processes 146.7 kt CO<sub>2</sub>/y and enables 100 MW of renewable energy storage. Cost-effectiveness could improve with cheaper electricity, longer lifespans,

and lower SOEC costs. However, halving renewable availability could double the payback period.

Lim et al. [67] examined hybrid methanol production from methane tri-reforming and AWE. The costs were 416.8 €/t for AWE, 424.3 €/t for PEM, and higher for SOEC, primarily due to stack replacement. Electricity and feedstock costs are the primary drivers for AWE and PEM. While all systems struggle to reach 20 % profit margins under current global conditions, PEM shows the best potential through improved efficiency and lifespan, leading to shorter payback periods.

Yousaf et al. [73] significantly reduced methanol production costs by integrating SOEC for hydrogen generation instead of alkaline electrolysis, reducing hydrogen-related CAPEX and operational expenditures (OPEX) by over 20 %. The authors optimise the process flowsheet through heat and energy integration, employ elevated reactor conditions (approximately 212 °C and 75 bar) to boost carbon dioxide conversion, and refine reactor design to minimise recycled streams and compression needs. Together, these strategies enhance efficiency, decrease energy demands, and lower the methanol production cost from approximately 908 €/t to around 599 €/t under optimal conditions.

The previously mentioned study by Emadi et al. [62] explored methanol production from carbon dioxide via DAC and SOEC, estimating levelized costs of 1.13 €/kg, double the fossil-based cost, and 2.38 €/kg for synthetic fuel. Environmental benefits are significant: methanol emits 31.1 gCO<sub>2-eq</sub>/MJ (22 % less), and synthetic fuel just 5.2 gCO<sub>2-eq</sub>/MJ (~ 6 times lower). Despite high capital costs, progress in SOEC and renewable integration supports long-term sustainability.

For ammonia, the scalability and compatibility of SOECs with the Haber-Bosch process offer promising prospects. A study by Nami et al. [68] comparing AWE and SOEC for green ammonia finds that AWE is currently cheaper; however, SOEC is expected to become more cost-competitive by 2050, given the improvement in electrolyser costs. At 30 €/MWh electricity, SOEC-based ammonia could reach 495 €/t. Lowering electricity prices from 60 to 10 €/MWh could reduce costs from 690 to 340 €/t.

SOECs offer high-temperature, high-efficiency electrolysis of steam and carbon dioxide, making them well-suited for hydrogen and syngas-based methanol production. Their economic feasibility depends on several interrelated technical, system-level, and market factors. One of those factors correspond to materials and stack design, where recent developments have focused on improving durability and reducing cost through advanced materials, such as alternative electrodes (e.g., lanthanum ferrites, perovskites)(which are more resistant to redox and thermal cycling), metal-supported cells (that allow for thinner, mechanically robust designs), and improved proton-conducting ceramics (with lower degradation rates and faster startups). This could improve efficiency and lifetimes (> 40,000 h) while reducing OPEX due to replacement components [74].

Another relevant factor is the co-electrolysis and methanol synthesis integration. The main advantage of this approach is that syngas can be converted into methanol with minimal post-processing. Methanol is typically synthesised from syngas over a Cu/ZnO/Al<sub>2</sub>O<sub>3</sub> catalyst at 50–100 bar and 200–300 °C. The ideal H<sub>2</sub>:CO ratio for this reaction is around 2:1. SOEC systems allow precise control of the H<sub>2</sub>:CO ratio through their operating parameters (e.g., temperature, steam/CO<sub>2</sub> feed ratio, current density), making the syngas directly suitable for methanol synthesis and removing the need for reforming, shift reactors, or CO separation, simplifying the overall process, lowering capital and energy costs. Moreover, co-electrolysis and methanol synthesis operate at elevated temperatures, enabling thermal integration. The generated heat from methanol synthesis can be recovered to preheat the SOEC feed gases, improving overall system energy efficiency, often reaching 65–70 % or higher (based on total input vs. methanol energy content). This coupling is more efficient than running electrolysis and methanol synthesis as separate, standalone units [49].

Manufacturing scale and cost reduction are also two very significant factors. Recent TEA studies show that SOEC stack costs could drop below

85 €/kW<sub>e</sub> with GW-scale manufacturing, which is significantly lower than the current small-scale production ( $\leq 1$  MW) stack costs (~683–1281 €/kW<sub>e</sub>) [75]. Moreover, system CAPEX can fall 30–40 % with supply chain maturity and design standardisation. This results in reduced hydrogen cost production of 1.7 €/kg, assuming an electricity cost of 0.02 €/kWh [76]. In most real-world SOEC deployments today, hydrogen production costs typically lie between 3.0 and 4.7 €/kg [77,78].

Thermal and electrical integration also represent a relevant factor concerning economic viability. SOECs benefit from coupling with waste heat, concentrated solar power, or nuclear heat, reducing power demand. Integration with methanol synthesis boosts efficiency, for instance, up to 30 % less electricity, with system efficiencies > 90 % (LHV) [79].

Moreover, SOECs have traditionally struggled with thermal cycling; however, new designs offer faster ramping, improved thermal shock resistance, and predictive maintenance, enabling flexible use with wind and solar. This improved design positively impacts the economic feasibility of SOECs since it increases the capacity factor and uses low-cost surplus electricity, lowering LCOH without needing expensive storage systems [75].

Lastly, policy and deployment issues, such as carbon pricing, green fuel rules (e.g., renewable fuels of non-biological origin, like green hydrogen or e-methanol), and public subsidies support SOEC scale-up, especially in hydrogen/methanol hubs near carbon dioxide and renewables, which improve competitiveness against the traditional fossil routes [80].

It is important to note that techno-economic results reported in the literature are not always directly comparable, since they are based on heterogeneous boundary conditions and assumptions. One of the most influential parameters is the electricity price, which is typically assumed between 20 and 60 €/MWh, though some studies use lower values (< 15 €/MWh) to represent surplus renewable electricity [65,71,73]. Another critical factor is the stack lifetime and replacement cycle, which can vary from 20,000 to 40,000 h, with replacement intervals assumed between 4 and 7 years [69,75]. The system scale also plays a decisive role, with costs reported for small laboratory stacks (kW) generally exceeding those for MW-scale demonstrations due to economies of scale [66,69]. Furthermore, differences in discount rates and financing assumptions (typically 5–10 %) affect the LCOH reported across studies [68,71]. Finally, the efficiency basis introduces another source of variation, since some authors report results on an LHV basis, while others use the higher heating value (HHV) or mixed conventions [68,79]. In this review, cost data have been normalised where possible to €/kg H<sub>2</sub> (for hydrogen production), €/kW (for CAPEX), and €/kWh (for electricity), but the values should be interpreted as indicative ranges rather than absolute benchmarks, given the methodological diversity observed in the literature.

### 3. Solid oxide fuel cells (SOFCs)

SOFCs are high-temperature electrochemical devices that convert the chemical energy of various fuels into electricity with high efficiency, low emissions, and a potentially long service life estimated between 40,000 and 80,000 h. Operating within a temperature range of 600 °C to 1,000 °C, SOFCs enable the direct use of multiple fuel types, such as hydrogen, NG, syngas, and biogas. This feature provides notable versatility for diverse energy applications [81,82].

A typical SOFC consists of a solid electrolyte that separates the anode from the cathode. The cathode functions as a reduction site, where oxygen molecules from the oxidant gas (air) are adsorbed and reduced to oxide ions. These ions migrate through the electrolyte, driven by a chemical potential gradient, towards the anode supplied with fuel [83]. There, the oxide ions catalytically oxidise the fuel, producing water, heat, and most importantly, electrons, which are used to perform useful work. The released electrons are then transported through an external

circuit back to the cathode, thus completing the electrochemical cycle. Fig. 3 illustrates a typical SOFC and its operating principles [83,84].

In addition to their fuel flexibility, SOFCs exhibit high electrical efficiencies, often exceeding 60 %, since Carnot cycle limitations do not constrain them due to their direct electrochemical conversion process. Low pollutant emissions also characterise them, as well as cost competitiveness compared to other fuel cell technologies, and modular scalability, which allows energy output to be adjusted by connecting multiple individual cells in series to meet specific power demands [81,85].

#### 3.1. Working principles and components

SOFCs are composed of three functional layers, namely, cathode, electrolyte, and anode, which are typically arranged in either planar or tubular configurations. The planar design offers higher power density but is more sensitive to thermal stress, while tubular and microtubular formats provide enhanced mechanical robustness and thermal cycling resistance. These electrochemical systems operate through coordinated reactions across their components, with all processes being exothermic and capable of achieving system efficiencies exceeding 85 % in CHP applications [86].

The cathode, typically fabricated from porous LSM or more advanced mixed ionic-electronic conductors (MIECs) such as LSCF and barium strontium cobalt ferrite (BSCF, Ba<sub>0.5</sub>Sr<sub>0.5</sub>Co<sub>0.8</sub>Fe<sub>0.2</sub>O<sub>3.δ</sub>), facilitates the oxygen reduction reaction. These materials enable both ionic and electronic conduction, thus extending the reactive area beyond traditional triple-phase boundaries and improving performance at intermediate temperatures [57,87].

The electrolyte layer, most commonly composed of dense YSZ, or scandia-stabilised zirconia (ScSZ, ZrO<sub>2</sub> doped with Sc<sub>2</sub>O<sub>3</sub>), serves the dual function of conducting oxygen ions toward the anode while preventing gas crossover. Alternative materials such as gadolinium-doped ceria (GDC, Ce<sub>1-x</sub>Gd<sub>x</sub>O<sub>2.δ</sub>) offer superior ionic conductivity at intermediate temperatures, though they may exhibit partial reduction under fuel exposure, potentially leading to undesirable electronic conduction [88].

At the anode, oxygen ions react with various fuel sources through distinct electrochemical pathways. The standard anode material consists of a Ni-YSZ cermet, which combines high electronic conductivity with ionic transport capabilities. However, due to susceptibility to carbon deposition and sulphur poisoning at lower temperatures, alternative materials, including Ni-GDC and perovskite oxides such as strontium iron molybdate (Sr<sub>2</sub>Fe<sub>1.5</sub>Mo<sub>0.5</sub>O<sub>6.δ</sub>) are under development [89,90].

The thermodynamic characteristics of these electrochemical reactions vary significantly depending on the fuel type employed [86]. Table 5 summarises the key reactions, their Gibbs free energy ( $\Delta G^\circ$ ) and enthalpy ( $\Delta H^\circ$ ) changes at standard conditions (298 K), along with their operational characteristics.

#### 3.2. Cost and performance considerations of SOFC systems

SOFCs have seen notable improvements in cost and durability, yet economic viability remains one of the major barriers to widespread deployment. In the short term, capital costs are still relatively high, particularly due to expensive materials (e.g., rare earth oxides, high-grade ceramics, and Ni-based cermets), complex manufacturing processes, and stack sensitivity to thermal cycling. For comparison, PEMFC systems currently achieve lower stack costs (~800–1,500 €/kW) due to their simpler manufacturing, though SOFCs offer superior electrical efficiency in CHP applications, supported by detailed modelling showing SOFC stack costs are typically higher, and the efficiency advantage is significant [91].

Current stack manufacturing costs are estimated at 1,000–3,000 €/kW, while the Balance of Plant (BoP), which includes fuel processors, inverters, heat exchangers, and control systems, adds 500–1,000 €/kW

**Table 5**  
Electrochemical reactions and thermodynamic parameters in SOFC systems.

Fuel	Overall reaction	$\Delta G^\circ$ (298 K) (kJ/mol)	$\Delta H^\circ$ (298 K) (kJ/mol)	Process description
Hydrogen	$H_2 + \frac{1}{2}O_2 \rightarrow H_2O$	-237.1	-241.8	Direct electrochemical oxidation of $H_2$ at the anode; cleanest and most efficient fuel.
Carbon monoxide	$CO + \frac{1}{2}O_2 \rightarrow CO_2$	-283.0	-283.0	$CO$ is electrochemically oxidised to $CO_2$ ; common in syngas and biogas applications.
Methane	$CH_4 + 2O_2 \rightarrow CO_2 + 2H_2O$	-802.3	-890.3	Requires internal reforming to $CO$ and $H_2$ before electrochemical oxidation.
Syngas	$CO + H_2 + O_2 \rightarrow CO_2 + H_2O$	-520.0	-525.0	Blend of $H_2$ and $CO$ from reforming processes; both components undergo oxidation.
Biogas	$CH_4 + CO_2 + 2O_2 \rightarrow 2CO_2 + 2H_2O$	-640 to -800	-800 to -890	Internal reforming of $CH_4$ with $CO_2$ acting as reforming agent (dry reforming).

depending on system scale and integration [92,93]. The Clean Hydrogen Partnership's SRIA includes a unit-cost Key Performance Indicator (KPI) of 500 €/kW for advanced high-temperature co-electrolyser technologies, while the International Energy Agency (IEA) forecasts installed electrolyser CAPEX falling below 1,000 \$/kW (~ 900–1,000 €/kW) by 2030, enabled by material innovation and automated production scale-up [94,95].

OPEX typically represents 3–6 % of the initial capital investment per year, though this can vary significantly based on fuel type, maintenance cycles, and system design. SOFC systems operating on pure hydrogen benefit from lower contaminant loads, resulting in less frequent maintenance and fewer component replacements. In contrast, systems using NG or biogas require more rigorous gas cleanup and periodic anode regeneration or replacement, which increases OPEX [92,96]. Recent advances in sulphur-tolerant Ni-GDC anodes, such as barium cerium ytterbium oxide - impregnated (BCYb,  $BaCe_{0.9}Yb_{0.1}O_{3-\delta}$ ) or nanostructured architectures, and complementary gas purification strategies have been shown to mitigate sulphur poisoning (e.g., up to 500 ppm  $H_2S$ ), substantially improving durability and reducing maintenance needs in hydrocarbon-fueled SOFCs, which can lead to OPEX reduction [97].

The Levelized Cost of Electricity (LCOE) is a key metric for assessing cost competitiveness, as it calculates the present value of the total cost of constructing and operating a power plant over its lifetime. It ranges from 0.25 to 0.35 €/kWh for small-scale residential or commercial SOFC systems (1–10 kW) and approaches 0.15 €/kWh for large-scale deployments (> 100 kW). With further scale-up, standardisation, and improvements in stack longevity, LCOE values could fall below 0.10 €/kWh, making SOFCs more competitive with CHP technologies and even grid electricity in some countries from the European Union (EU) [98,99]. At industrial scale (> 250 kW), SOFC-CHP installations can reach LCOE parity or outperform NG turbines in regions where electricity prices exceed ~ 0.20 €/kWh (spark spread ~ 0.10 €/kWh), assuming stack CAPEX near 1,200 €/kW and moderate lifetime (~5 years), with modelled electricity cost reductions of up to ~ 46 % [100].

Durability remains a challenge, with commercial systems offering lifetimes ranging from 20,000 to 40,000 h under real operating conditions. Degradation phenomena such as nickel coarsening, chromium poisoning from interconnects, and delamination at material interfaces are key factors that reduce efficiency and require performance optimisation strategies [92,101]. Mitigation approaches include chromium-blocking spinel coatings (e.g., Mn-Co-Fe spinel on interconnects providing > 40,000 h stability) and nanostructured Ni-YSZ anodes that inhibit Ni coarsening (> 60,000 h projected performance) as shown by advanced phase-field studies and tomography [102,103]. Table 6 presents a summary of the cost and performance metrics of SOFCs.

To complement the detailed data presented in Tables 4 and 6, Fig. 5 provides a radar chart comparison of AWE, PEM, AEM, SOEC, and SOFC technologies across five key performance metrics: CAPEX, OPEX, lifetime, efficiency, and technology readiness level (TRL). The visualisation highlights the trade-offs between mature low-cost technologies such as AWE and PEM, which offer high TRL and strong load flexibility, and

**Table 6**  
Key cost and performance metrics for SOFC systems.

Category	Metric / Range	Notes	Ref.
CAPEX	1,500–4,000 €/kW	Stack: 1,000–3,000 €/kW; BoP: 500–1,000 €/kW	[94,95]
OPEX	3–6 % of CAPEX per year	Lower with hydrogen; higher with methane/ biogas due to impurities and maintenance	[94,98]
LCOE (1–10 kW systems)	0.25–0.35 €/kWh	Residential, low-scale CHP	[100,101]
LCOE (100–250 kW)	~0.15 €/kWh (0.10 €/kWh with scale)	Industrial-scale deployment, cost decline expected	[94,95]
Lifetime	20,000–40,000 h	Real-world performance	[94,103]
Degradation mechanisms	Ni coarsening, Cr poisoning, delamination	Affects durability and power output	[94,98]

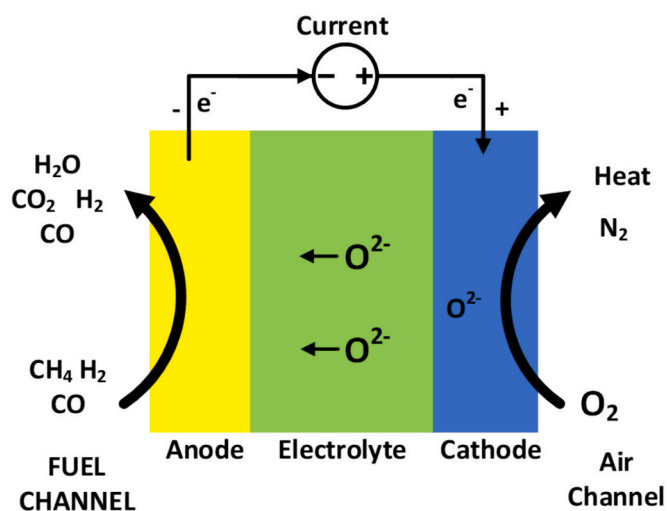


**Fig. 4.** Schematic diagram highlighting key features of SOFC operation.

emerging options like AEM and SOEC, which demonstrate promising efficiency or material advantages but remain limited by lower durability and higher cost structures [59,70,75,91,94]. SOFCs show strong efficiency potential, particularly in combined heat and power (CHP) applications, but their relatively high CAPEX and moderate lifetimes continue to limit widespread adoption.

While both SOECs and SOFCs remain cost-prohibitive compared to AWE and PEM, ongoing advances in material innovation (e.g., alternative electrodes, reduced rare-earth content, improved degradation resistance) and manufacturing scale-up could significantly reduce costs and extend lifetimes. Reaching long-term targets of < 0.10 €/kWh LCOE and > 60,000 h durability will require continued progress in stack

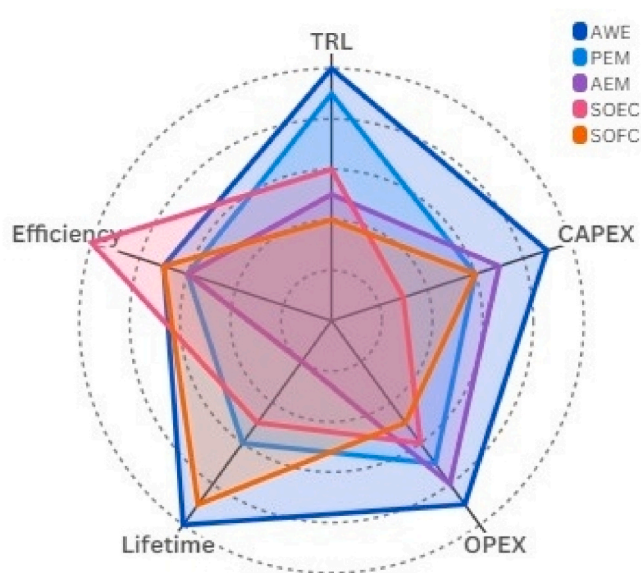


Fig. 5. Multi-criteria comparison of SOFCs with other electrolysis and fuel cell technologies.

design, predictive maintenance, and system-level integration strategies [73–75,92,98,102].

### 3.3. Material innovations

Perovskite oxides have emerged as promising alternatives to Ni-based SOFC anodes owing to their chemical stability in reducing atmospheres, resistance to coking and sulphur poisoning, and reduced redox-induced volume changes. Among them,  $\text{La}_{0.7}\text{Sr}_{0.25}\text{Cr}_{0.5}\text{Mn}_{0.5}\text{O}_3$  (LSCrM) exhibits notable redox robustness, though with lower conductivity than conventional Ni–YSZ. Its performance can be enhanced by impregnating secondary metals such as Cr, Sc, Ti, Nb, or Bi, which increase electronic transport, oxygen vacancy concentration, and catalytic activity [104–107]. For instance, Co impregnation increased LSCrM power density in YSZ-supported cells more than threefold, while Bi doping enabled stable 50 h operation at 800 °C under  $\text{CH}_4$  without coking [104].

Antolini [108] reported liquid metal anodes as another promising route, with molten antimony (Sb) showing excellent durability and performance. In these systems, Sb oxidises to  $\text{Sb}_2\text{O}_3$  at the electrolyte interface and is then reduced by carbon, maintaining continuous hydrocarbon conversion. This redox cycle yields low interfacial resistance ( $0.06 \Omega \text{ cm}^2$ ), high power output (up to  $360 \text{ mW/cm}^2$ ), and long-term stability exceeding 650 h in sulphur-containing kerosene without coking [109]. Compared with other liquid metals such as Sn or Bi, Sb displays lower polarisation losses and higher open-circuit voltage ( $\sim 0.75 \text{ V}$  at 700 °C). Horizontal tubular flow fields further stabilise the Sb/ $\text{Sb}_2\text{O}_3$  phase distribution, improving voltage stability during extended operation [107,108].

Palladium-based strategies (PdO impregnation and Pd doping) have also shown strong potential to enhance electrochemical activity, even in large-area single cells. Pd incorporation increases surface activity, reduces interfacial resistance, and optimises cathode microstructure, though high-temperature sintering and agglomeration remain challenges. Stabilisation through alloying or secondary phases effectively suppresses PdO growth and maintains durability [110].

Li et al. [111] synthesised  $\text{La}_{0.1}\text{Sr}_{1.9}\text{Fe}_1$ ,  $4\text{Ni}_{0.1}\text{Mo}_{0.5}\text{O}_{6-\delta}$  (LSFNM) and  $\text{Pr}_{0.1}\text{Sr}_{1.9}\text{Fe}_1$ ,  $4\text{Ni}_{0.1}\text{Mo}_{0.5}\text{O}_{6-\delta}$  (PSFNM) Ruddlesden–Popper oxides with exsolved  $\text{FeNi}_3$  nanoparticles to improve sulphur tolerance. La doping reduced polarisation resistance by 44 %, with single-cell power densities of  $1.37 \text{ W/cm}^2$  in  $\text{H}_2$  and  $1.31 \text{ W/cm}^2$  in 50 ppm  $\text{H}_2\text{S-H}_2$  at

850 °C. PSFNM showed superior sulphur resistance, maintaining performance over repeated  $\text{H}_2/\text{H}_2\text{S}$  cycles.

Rahumi et al. [112] investigated Ni-doped  $\text{Sr}_{1.9}\text{Fe}_{1.5-x}\text{Ni}_x\text{Mo}_{0.5}\text{O}_{6-\delta}$  anodes decorated with exsolved  $\text{FeNi}_3$  nanoparticles for ammonia-fuelled SOFCs. Optimised Ni doping delivered  $516 \text{ mW/cm}^2$  at 800 °C, 99.6 % ammonia conversion,  $0.15 \Omega \text{ cm}^2$  polarisation resistance, and 39.7 % electrical efficiency.

Overall, incorporating secondary metals such as Ni, La or Co into perovskite structures markedly enhances SOFC performance by promoting the exsolution of active  $\text{FeNi}_3$  nanoparticles. This synergistic effect improves catalytic activity, conductivity, and sulphur tolerance, confirming multi-metal doping as an effective route to high-performance, durable SOFC anodes.

## 4. Reversible solid oxide cells (rSOCs)

### 4.1. Working principles and system configuration

rSOCs represent an integration of SOFC and SOEC technologies, maintaining structural identity with conventional SOFC systems while enabling dual-mode operation. These systems can operate either as fuel cells to convert chemical energy from hydrogen-rich fuels (such as syngas, ammonia, or NG) directly into electricity when energy prices are high (Fig. 4) or as electrolyzers utilising excess electricity and waste heat to produce hydrogen during periods of low electricity [113–116].

Reversible operation provides significant advantages over conventional systems, mainly through the elimination of separate units for power generation and hydrogen production. The system's performance critically depends on electrode materials that can maintain functionality under alternating operational modes. The oxygen electrode, serving as a cathode during SOFC operation and an anode during SOEC operation, presents challenges due to its higher polarisation losses in electrolysis mode [117,118]. Likewise, the hydrogen electrode must accommodate varying fuel compositions and operational conditions [113–116].

One of the technical and economic aspects to consider in rSOC technologies is the materials used in their manufacture, as they play a key role in determining the total cost of the stack or individual cells and their subsequent performance. For the SOEC module, commonly used electrolyte materials include YSZ, typically with 8 mol% yttria, scandia-stabilized zirconia (ScSZ), generally containing 9 mol% scandia ( $\text{Sc}_2\text{O}_3$ ), and GDC. In the SOFC module, the fuel electrode typically comprises a NiO–YSZ composite, while the oxygen (or air) electrode is usually made of LSM or LSCF [114,116]. Further details regarding the materials used in rSOCs can be found in Table 1.

When compared to traditional AWE and PEM electrolyzers, rSOCs demonstrate superior performance characteristics. Their high operating temperatures (600–850 °C) provide thermodynamic advantages, significantly reducing the electrical energy required for electrolysis. Furthermore, rSOCs offer greater fuel flexibility compared to PEM systems, which require extremely pure hydrogen feedstock. The integrated design of rSOC systems reduces both CAPEX and operational complexity associated with maintaining separate power generation and hydrogen production units [1,114,115,119].

These operational and design advantages position rSOC technology as particularly suitable for renewable energy integration, offering simultaneous solutions for energy storage through hydrogen production and dispatchable power generation within a single system [114,116].

### 4.2. Cost and performance considerations of rSOC systems

rSOCs, though less mature than PEM and AWE technologies, are advancing rapidly as a promising high-efficiency alternative with potentially lower capital costs. Their higher operating temperatures enable efficient operation at thermoneutral voltage conditions, which is particularly beneficial for SOEC [120].

Recent TEA studies have quantified rSOC performance and viability.

For example, Parashar et al. [120] developed a comprehensive 1 MW<sub>AC</sub> system model interfaced with hydrogen infrastructure, demonstrating 54.1 % hydrogen production efficiency with a baseline LCOH of 2.74 €/kg. Their analysis identified electricity costs as the primary economic driver, with potential LCOH reduction to 1.87 €/kg under favourable electricity price arbitrage conditions. The study revealed distinct cost structures for different operational modes, with current stack costs estimated at 273 €/kW for SOEC and 472 €/kW for SOFC operation. Complementing these findings, Liang et al. [121] evaluated an integrated rSOC-PV (photovoltaic) system, reporting a LCOE of 0.1253 €/kWh alongside hydrogen production at 3.84 €/kg, with an 11-year project payback period. The economic assessments reveal consistent cost structures across implementations. Fixed operation and maintenance (O&M) costs, representing 15–18 % of total expenditures, account for periodic stack replacement (assuming a 5 year/40,000 h lifespan) and BoP maintenance. Variable O&M costs account for 67 % of total costs, primarily driven by electricity consumption during electrolysis operation. CAPEX concentrates heavily on the stack (45 %) and heat exchangers (42 %), reflecting the system's dependence on advanced thermal management for efficient heat recuperation.

Operational strategies emerging from these studies emphasise dual-mode optimisation: utilising low-cost excess renewable electricity during electrolysis operation while capitalising on peak electricity prices during fuel cell operation. This arbitrage approach, combined with careful thermal management, has a significant impact on the overall system economics. The integrated analysis by Liang et al. [121] further demonstrates the long-term viability of such systems, showing positive net present value after the 11th year of operation, accumulating to approximately 3,127,540 € over the 20-year system lifetime. Table 7 synthesises cost and performance benchmarks, emphasising this technology's scalability and future cost-reduction pathways.

As with SOEC systems, it should be emphasised that reported techno-economic data for rSOCs are strongly dependent on assumptions regarding electricity price, stack lifetime, and system scale. Therefore, the values presented here should be interpreted as indicative ranges rather than absolute benchmarks, consistent with the discussion in Section 2.5.2.

#### 4.3. Material innovations and system control strategies

The development of rSOCs has been driven by parallel advancements in three critical areas: novel electrode materials enabling stable

**Table 7**  
Summary of rSOCs cost and performance metrics.

Category	Metric / Range	Notes	Ref.
CAPEX	~1,370 €/kW	rSOC price in €/kW: 1250 (2030) and 500 (2050) Storage price in €/kWh: 8 Compressor price in €/kW: 100 rSOC lifetime (stack) in years: 10	[109,113]
	~1,660 €/kW	Stack costs for SOEC and SOFC modes are 273 €/kW and 472 €/kW, respectively, while the system costs for SOEC and SOFC modes are 608 €/kW and 1051 €/kW, respectively	[113]
	6,986,020 €	Prices of rSOC (892,623 €), PV modules, turbines, heaters, pumps, etc	[114]
OPEX	18 % of LCOH/y 419,160 €/y	However, variable O&M costs can represent 67 % of LCOH 6 % of CAPEX (6,986,020 €)	[113] [114]
LCOH	~1.87 – 2.74 €/kg	Industrial scale deployment, cost decline expected	[24,113]
LCOE	0.1253 €/kWh	Industrial scale	[114]
Lifetime	40,000 h	Real-world performance	[113]

operation under alternating redox conditions, sophisticated control strategies for managing complex mode transitions, and system-level integration approaches that maximise efficiency and durability. Together, these innovations are overcoming barriers to rSOC commercialisation while creating new opportunities for grid-scale energy storage and sector coupling.

Material innovation has addressed one of the most fundamental challenges in rSOC development, namely, creating electrodes capable of maintaining high activity for both oxygen reduction and oxygen evolution reactions. Martsinchyk et al. [122] demonstrated the system-level benefits of advanced materials through their innovative integration of SOFC stacks with molten carbonate fuel cells (MCFCs) in a power-to-gas (PtG) configuration. This hybrid approach achieved remarkable 60–80 % round-trip efficiencies while simultaneously enabling carbon dioxide capture and utilisation, a critical capability for carbon-neutral energy systems. The success of this design stems from its closed-loop operation, where the MCFC effectively manages thermal and material flows between components, demonstrating how material selection impacts overall system performance.

At the nanoscale level, significant progress has been made in composite electrode architectures. Wang et al. [123] developed a breakthrough GDC with praseodymium barium strontium cobaltite coating (GDC@PBSC, Ce<sub>0.9</sub>Gd<sub>0.1</sub>O<sub>2.8</sub>@PrBa<sub>0.5</sub>Sr<sub>0.5</sub>Co<sub>2</sub>O<sub>5.8</sub>) oxygen electrode using a one-pot molten salt synthesis method. This unique design anchors nano-sized GDC particles onto larger PBSC substrates, creating an extended three-phase boundary that enhances both ionic conductivity and catalytic activity. When tested in practical SOC operation, the composite demonstrated exceptional performance metrics: 0.64 W/cm<sup>2</sup> power density in fuel cell mode and 0.40 A/cm<sup>2</sup> current density in electrolysis mode at 750 °C. These values represent 25–30 % improvements over conventional electrodes, while the reduced thermal expansion coefficient (TEC) minimises delamination risks during thermal cycling. Complementing these material advances, simplified fabrication techniques are lowering manufacturing barriers. Rehman et al. [124] introduced an innovative infiltration method using trichloroacetic acid that eliminates the need for repeated high-temperature calcination steps. Their approach produces nanostructured lanthanum cobaltite (LaCoO<sub>3</sub>) electrodes with excellent phase purity and adhesion to GDC scaffolds. Most impressively, these electrodes maintained stable performance through over 100 operational cycles between SOFC and SOEC modes, showing no detectable degradation at 750 °C. This durability milestone is particularly significant for commercial applications where frequent cycling is required.

Yang et al. [125] reported that rare-element-doped perovskites, double perovskites, and Ruddlesden–Popper structures enhance catalytic activity, resistance to poisoning, and long-term stability in reversible SOCs. Advanced fabrication methods such as electrophoretic deposition, plasma spraying, electrospinning, exsolution, and barrier-layer coatings further suppress degradation. Symmetrical electrode designs mitigate thermomechanical mismatch, while optimising operating parameters (temperature, current density, gas supply, and switching protocols) improves durability and round-trip efficiency. Composite bifunctional materials improve redox stability and resistance to coking and sulphur poisoning. For fuel electrodes, La-doped SrTiO<sub>3</sub> (LST) shows strong carbon and sulphur tolerance, while Ni–BSCY suppresses SDC reduction and achieves higher open-circuit voltage and current density than Ni–SDC or Ni–YSZ. For oxygen electrodes, Ruddlesden–Popper oxides (e.g., La<sub>2</sub>NiO<sub>4+δ</sub>) and double perovskites such as PBMO, PBSCF, PBCO, and SFMO offer superior ionic/electronic conductivity and catalytic activity compared with conventional perovskites [125–127].

S.W. Lee et al. [128] developed a Ni–Fe bimetallic fuel electrode decorated with nanosized ceria via a solid injection–ultrasonic spraying (SDI–USSP) process. The ceria nanodots exhibit strong oxygen-trapping ability and promote oxygen-ion migration, while a dense La-doped ceria barrier layer suppresses Ni diffusion into the LSGM electrolyte. The in situ formation of convex CeO<sub>2</sub> nanodots enhances ionic conductivity,

enabling a peak power density of  $1.40 \text{ W cm}^{-2}$  at  $800 \text{ }^\circ\text{C}$  and an electrolysis current density of  $1.01 \text{ A cm}^{-2}$  at  $1.3 \text{ V}$ , with stable operation for 500 h.

The development of advanced control systems has been equally critical for achieving practical rSOC operation. Liu et al. [129] created a comprehensive 1D model that simulates transient behaviour during mode switching, identifying key safety limits for commercial deployment. Their work stated that current changes must remain below  $7 \text{ A/s}$  to prevent fuel starvation, while temperature gradients exceeding  $5 \text{ K}$  can accelerate material degradation. To manage these constraints, the authors implemented a dual-model predictive control (DM-MPC) strategy that dynamically adjusts operating parameters during transitions. This approach reduced thermal stresses by  $40 \%$  compared to conventional proportional-integral-derivative (PID) controls, while maintaining system efficiency.

For larger-scale implementations, Xu et al. [130] developed a hybrid model predictive control (MPC) system for  $5 \text{ kW}$  rSOC units. Their strategy combines feedforward control with MPC feedback to precisely regulate stack temperatures during current variations. Experimental validation demonstrated that the thermal overshoot was limited to  $2.3 \text{ K}$  (a  $60 \%$  reduction), while transient efficiency was improved by  $5\text{--}8 \%$ . The system also demonstrated faster response times ( $100\text{--}2500 \text{ s}$ ) and  $1\text{--}3 \%$  higher steady-state efficiency compared to traditional controls. These advances are particularly valuable for integrating renewable energy, where rapid response to fluctuating power inputs is essential.

Long-term degradation management represents the third critical innovation area for rSOC viability. Califano et al. [131] addressed this challenge through hierarchical control strategies tested in polygeneration microgrid simulations. Their limited grid support (LGS) approach kept  $90 \%$  energy self-sufficiency even under aggressive degradation rates of  $1 \%/ \text{kh}$  over a 3-year continuous operation. This was achieved by balancing rSOC utilisation with auxiliary systems while prioritising hydrogen storage state-of-charge (SoC) as a key metric. The strategy proved particularly effective at mitigating the cumulative impacts of redox cycling and thermal stress.

## 5. Benchmarking commercial readiness: Worldwide SOC projects and demonstration initiatives

### 5.1. SOEC demonstrations

SOEC demonstration units have garnered attention in recent years, aiming to establish reliance and demonstrate the technology's effectiveness in promoting its scalability for large-scale hydrogen production. Compared to other electrolysis technologies, SOEC is one step behind in terms of technology maturity, with a strong state-of-the-art system developed in recent years through innovation projects [71]. As summarised in Table 8 (SOEC demonstration projects).

The initiatives described in Table 8 demonstrate three critical aspects of technological advancement: operational validation at increasing scales, efficiency improvements through high-temperature operation,

and successful integration with industrial processes.

Topsoe's  $350 \text{ kW}$  system validation [132] and Bloom Energy's rapid deployment of a  $4 \text{ MW}$  electrolyser [133] represent important milestones in proving the reliability of SOEC systems at near-commercial scales. These projects have achieved continuous operation periods exceeding  $2,250 \text{ h}$  while maintaining stable performance, addressing concerns about the technology's operational durability. The efficiency advantages of high-temperature operation are particularly evident in Bloom Energy's system, which demonstrates  $20\text{--}25 \%$  higher hydrogen production rates compared to conventional low-temperature electrolysers.

Sunfire's diverse project portfolio provides compelling evidence of the technology's adaptability across different applications. The company's work on pressurised SOEC systems for the HELMETH project achieved  $90 \%$  steam conversion rates at  $15 \text{ bar}$  pressure [134,135].

The progression from laboratory-scale to MW-scale demonstrations indicates accelerating technology maturation. Topsoe's construction of a  $500 \text{ MW}$  manufacturing facility [136] and Bloom Energy's planned  $1.8 \text{ MW}$  deployment in South Korea [137] suggest growing industry confidence in SOEC technology. However, challenges remain in achieving full commercial viability, particularly regarding stack lifetime limitations (typically  $40,000 \text{ h}$ ) and the need for further cost reductions through economies of scale.

These projects suggest that SOEC technology is transitioning from the research and development phase to pre-commercial deployment. The successful validation of various system configurations and operating modes provides a strong foundation for future scale-up efforts, though continued work on durability enhancement and cost reduction will be essential for widespread commercial adoption.

### 5.2. SOFC demonstrations

The EU is accelerating its low-carbon transition by funding SOFC development through the Clean Hydrogen Joint Undertaking, among other funding mechanisms like Horizon Europe, Innovation Fund, Important Projects of Common European Interest (IPCEI) or the LIFE-Clean Energy Transition [138–142]. Initiative from the Clean Hydrogen Joint Undertaking mainly targets fossil fuel displacement by advancing fuel cells for hydrogen, biogas, and syngas applications across multiple sectors, including CHP, maritime propulsion, and reversible systems for energy storage. Table 9 summarises the main objectives, geographical scope, and TRL targets of a few of these projects.

Alongside EU-funded projects, several manufacturers worldwide have deployed SOFC systems at pilot and commercial scales. Table 10 highlights key systems, demonstrating the technology's progression toward diverse applications.

While EU projects focus on advancing TRL, commercial deployments (e.g., Bloom Energy, Mitsubishi) validate operational reliability. However, challenges persist in scaling production and reducing stack degradation, which ongoing research aims to address. SOFC demonstration units are field-deployed systems that aim to showcase the

**Table 8**  
Summary of global SOEC demonstration projects.

Company	Project	Scale	Key Metrics	Year	Ref.
Topsoe	Frederikssund Test Center	$350 \text{ kW}$	$> 2,250 \text{ h}$ stable operation	2023	[121]
Topsoe	Haldor Topsøe Vj2 Factory	$500 \text{ MW}$ (planned)	Production capacity from 2025	2022–2025	[122]
Bloom Energy	NASA Ames Research Center	$4 \text{ MW}$	$2.4 \text{ t/d H}_2$ ( $20\text{--}25 \%$ $\uparrow$ efficiency vs. low-temp)	2023	[123]
Bloom Energy	Jeju Island Project	$1.8 \text{ MW}$ (planned)	Industrial-scale deployment	2025	[124]
Sunfire	HELMETH Project	$10 \text{ kW pSOEC}$	$90 \%$ steam conversion at $15 \text{ bar}$	2014–2016	[112,125]

**Table 9**  
Summary of EU projects focused on SOFC technologies [133–140].

Project	Country	Duration	Description & Expected TRL
HELENUS	Germany (DLR)	2022–2027	500 kW SOFC for cruise ship. Demonstration TRL 7 → 8.
SO FREE	Italy, with ENEA, and from Portugal (INEGI)	2021–2024	Modular SOFC-CHP on biomethane/H <sub>2</sub> . Prototype TRL 6 → 7.
DEMOSOFC	Italy (Turin)	2015–2020	110 kW pilot plant using biogas; real-world operation completed.
ComSos	Various (Clean Hydrogen)	2018–2020	SOFC-CHP systems from 10–60 kW in real settings; industrial strengthening.
PROMETEO	Spain, Italy	2021–2024	25 kW solar-powered SOE, TRL 5 (electrolysis).
TriSOFC	United Kingdom, Portugal (INEGI)	2012–2015	Low-temperature SOFC (LT-SOFC) of 1.5 kW for buildings; TRL 4 → 5.
Hy SPIRE	Poland and others	2024–2027	Flexible SOE electrolysis at < 700 °C, balanced ion and proton transport, TRL 4 → 6.
RUBY	Pan-European	2020–2024	Monitoring system for SOFC/PEMFC, diagnostics and reliability, TRL 5.

technology's performance, efficiency, and practicality while collecting real-world data. These units are used in various applications, including micro-combined heat and power ( $\mu$ -CHP), CHP, and stand-alone power generation as auxiliary power units (APUs) [143]. In recent decades, several studies have focused on developing SOFC technology to address issues such as the decentralisation of clean energy production. Fig. 5 shows some examples of demonstration units of SOFC technologies developed in recent years.

The development of SOFC technology has been demonstrated through numerous pioneering projects since the late 1990 s, showcasing its evolution from laboratory prototypes to near-commercial systems. The first major milestone came in 1998 when Siemens Westinghouse Power Corporation (SWPC) installed a 100 kW tubular SOFC system in Westervoort, Netherlands, achieving 60–70 % efficiency using NG [144]. This was followed by a 250 kW outdoor installation at BP's Alaska facility in 2003, marking important progress in scaling up the technology [145].

The following decade saw the diversification of SOFC applications. In 2010, Versa Power Systems developed a 10 kW stack that successfully operated for over 1,500 h with 60 % DC efficiency when tested at Finland's VTT Technical Research Centre [146]. European research initiatives such as the FC-DISTRICT project demonstrated micro-CHP

**Table 10**  
Overview of leading commercial and pilot-scale SOFC systems worldwide.

SOFC system	Power output	Electrical efficiency	Fuel type	TRL	Notes	Ref.
Bloom Energy Server (USA)	200–300 kW (modular)	50–60 % (up to 85 % CHP)	NG, Biogas	9	Commercial deployment in large facilities and data centres	[141]
Convion C50 (Finland)	50 kW	55–60 %	NG	8–9	Modular system, often integrated with heat recovery	[142,143]
SOLIDpower BlueGEN (EU)	1.5 kW	~ 60 %	NG	9	Residential/small commercial applications	[144]
Nexceris NexTech (USA)	1–10 kW	~ 60 %	Hydrogen, NG	6–7	Pilot scale, hybrid system compatibility	[145]
Mitsubishi MEGAMIE (Japan)	250 kW – 1 MW	55 – 65 %	NG, Biogas	8–9	Used in CHP microgrid systems	[146]

capabilities, with systems delivering 1.5–2.0 kW of electrical output and achieving up to 90 % overall efficiency when configured for trigeneration (power/heat/cooling) [147,148]. A particularly innovative application emerged in 2016 with the first European SOFC APU for heavy-duty trucks, achieving 30 % efficiency using conventional diesel fuel through an onboard reforming process [149].

Recent years have witnessed significant advances in system integration and environmental performance. Nabavi et al. [150] developed a novel kW-scale SOFC-integrated calciner that simultaneously generates electricity while capturing CO<sub>2</sub> through carbonate looping, demonstrating negative-emission potential. Hybrid configurations showed promise, with Kim et al. [151] reporting an 8 % efficiency boost in a 5 kW SOFC-engine system using hydrogen and reformed methane. The EU-funded DEMOSOFC project marked a milestone in 2020 by operating Europe's first industrial biogas-fed SOFC plant (174 kWe) at a wastewater treatment facility, consistently achieving 48–50 % efficiency from biogas to AC power [152].

Current demonstrations focus on hydrogen integration and large-scale deployment. The 2024 Erkelenz project combines SOFC with Liquid Organic Hydrogen Carrier (LOHC) technology to progressively transition from NG to hydrogen while supplying energy to a German hospital [153,154]. SolydEra's BlueGen 15 2.0 system (2024) demonstrates multi-fuel capability (NG, hydrogen, biomethane) with 89 % overall efficiency [155]. Most ambitiously, American Electric Power and Bloom Energy announced plans in 2024 to deploy up to 1 GW of SOFC capacity for data centres, beginning with 100 MW in 2025, with eventual hydrogen integration [156].

### 5.3. rSOC demonstrations

Recent demonstration projects have validated the rSOC system's unique capabilities for grid balancing and sector coupling applications. As part of the HELMETH project, Sunfire, in collaboration with Boeing, produced a grid-connected rSOC system capable of flexible operation between power generation and hydrogen production modes. On the other hand, the GrInHy project's integration of a 150 kW<sub>AC</sub> rSOC system into steel manufacturing processes at Salzgitter represents a major step toward practical industrial applications, achieving hydrogen production rates of 50 Nm<sup>3</sup>/h for steel annealing processes [16,119,157]. The SWITCH project (2018–2024), conducted in Italy, Switzerland, and Spain, focuses on advancing an rSOC system for continuous hydrogen production and flexible power generation. Aiming to raise the TRL from 6 to 7, this project demonstrates the system's performance in operational environments, marking a step toward commercial deployment [158]. Table 11 summarises details on the previously described projects.

To complement the detailed data provided in Tables 8 and 11, Fig. 7 summarises the timeline and scale of SOEC and rSOC demonstration projects between 2014 and 2025 [12,130,139–143,158]. The visualisation highlights the progression from early pilot-scale installations (< 200 kW) such as the HELMETH project [130–143] to recent and planned large-scale deployments in the multi-megawatt and even gigawatt

**Table 11**  
Summary of global rSOC company demonstration projects.

Company	Project	Scale	Key Metrics	Year	Ref.
Sunfire/ Boeing	Grid-Tied rSOC System	50 kW SOFC / 120 kW	3.5 kg H <sub>2</sub> / h + energy storage	2015–2017	[112,125]
Sunfire	GrInHy Project (Salzgitter)	SOEC 150 kW <sub>AC</sub>	50 Nm <sup>3</sup> /h H <sub>2</sub> for steel annealing	2019	[16]
–	SWITCH	50 kW SOFC/ 100 kg/ d H <sub>2</sub> in SOEC	40 kg/d of H <sub>2</sub>	2018–2024	[162]

range, including Bloom Energy’s 4 MW NASA Ames system [141] and Topsoe’s planned 500 MW Vj2 factory [141]. While SOEC technology has already achieved multi-MW demonstrations, rSOC projects remain smaller ( $\leq 150$  kW), exemplified by the GrInHy [16] and SWITCH initiatives [158], reflecting their earlier stage of development. The figure underscores both the rapid industrial scale-up of SOEC systems and the emerging maturity of reversible configurations.

Furthermore, several research papers focus on some pilot/industrial-scale works. Reznicek et al. [159] demonstrated a 50 MWe industrial-scale system operating at intermediate temperatures (600 °C) and high pressures (10–20 bar). This configuration leverages mild exothermic reactions to achieve two key benefits: eliminating external heat requirements during electrolysis and enhancing methane output for compatibility with existing gas infrastructure. The system’s bidirectional operation enables both power generation (with 90 % carbon dioxide capture) and synthetic fuel production through co-electrolysis.

For distributed applications, Perna et al. [160] developed a 100–200 kW hydrogen-based electric energy storage (HEES) system featuring breakthrough thermal integration. Their design eliminates external heat sources through optimised internal recovery, achieving 60 % round-trip efficiency and 91 % CHP efficiency. The team’s innovative thermo-electrochemical model enabled precise system optimisation while maintaining compact form factors suitable for decentralised deployment.

These implementations confirm the readiness of rSOC technology for dual-service applications. However, the need for extended durability testing under real-world cycling conditions and the cost reductions in stack manufacturing through scaled production remain ongoing barriers to overcome.

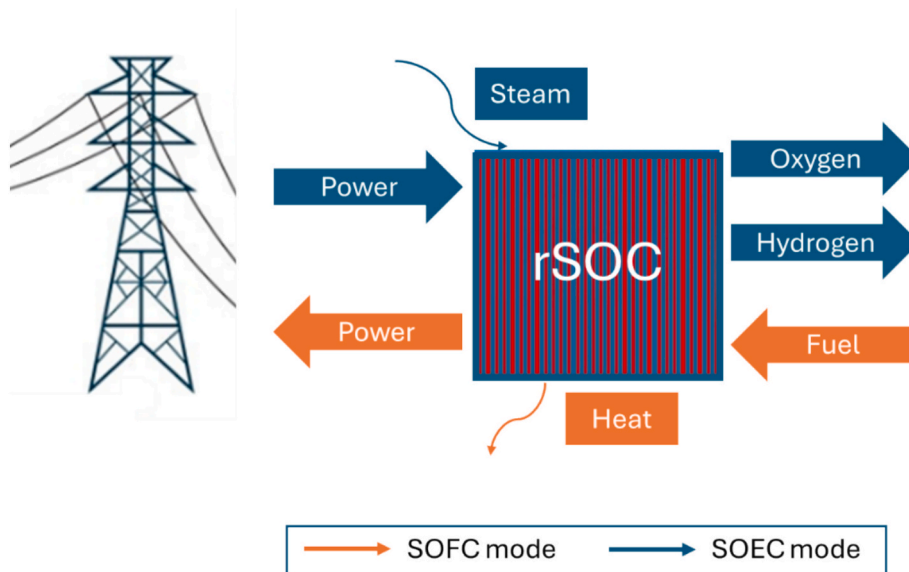


Fig. 6. Schematic diagram of rSOC operation modes.

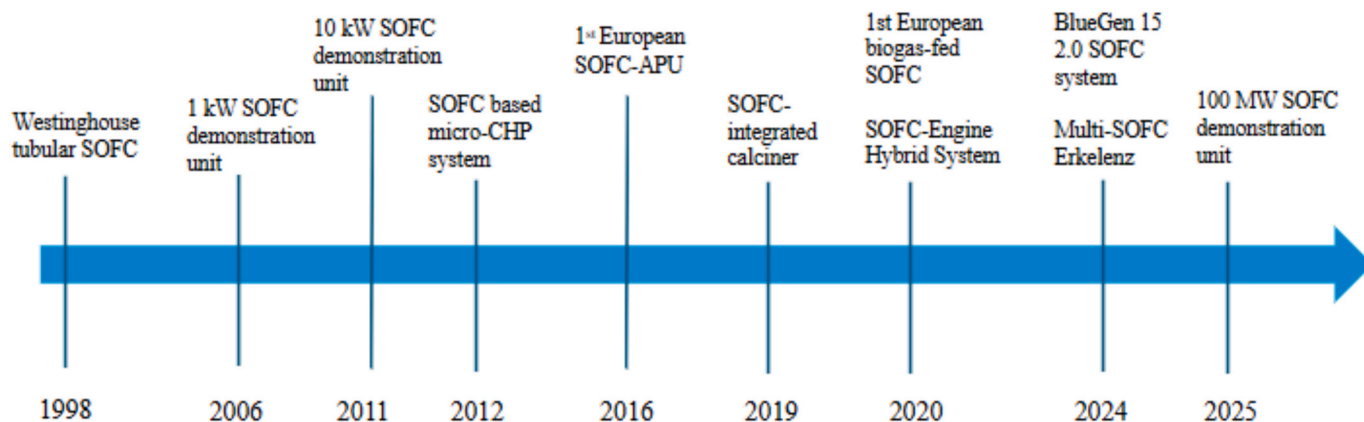


Fig. 7. Timeline for SOFC demonstration units in the last years.

## 6. SWOT analysis and future perspectives

Although SOEC is primarily an electrolysis technology and not a power generation system like SOFC, all three, SOEC, SOFC, and rSOC, are based on the SOC platform. A SWOT analysis (Fig. 6) was conducted to assess their relative technical maturity, system integration potential, and economic competitiveness within emerging hydrogen and energy storage markets (Figs. 8 and 9).

SOECs are increasingly recognized as one of the most efficient electrolysis technologies due to their high operational temperatures, which significantly reduce the electrical energy required for water splitting. Recent demonstrations, such as the one conducted by Fan et al. [161], detail how infiltration of strontium ferrite ( $\text{SrFe}_2\text{O}_{4-\delta}$ ) into LSM/YSZ air electrodes shows marked improvements in both hydrogen production efficiency and structural stability, effectively mitigating catastrophic delamination commonly observed in conventional SOEC stacks. Despite these advancements, large-scale deployment remains constrained by degradation mechanisms such as oxygen electrode instability, chromium vapour contamination, and electrochemical grain boundary effects under prolonged current, as stated by Dong et al. [162]. According to Han et al. [163], future research should prioritise the development of scalable MW-class stacks, the integration of process heat from sources such as concentrated solar and nuclear energy, and a systematic study of long-duration performance (over 20,000 h) under real-world dynamic conditions.

SOFCs continue to present one of the most promising solutions for high-efficiency, low-emission power generation, as described throughout this work. Innovations in cathode enhancement strategies, such as atomic layer deposition of zirconia as strontium getters, have demonstrated notable improvements in long-term electrochemical stability [164]. Similarly, nano-engineered cathode architectures, such as samarium-doped ceria interlayers, as tested by Machado et al. [165], have demonstrated durable performance at  $1 \text{ A/cm}^2$  and  $750 \text{ }^\circ\text{C}$ , with minimal degradation over 1,500 h. Future development should focus on intermediate-temperature operation ( $500\text{--}650 \text{ }^\circ\text{C}$ ) to reduce material costs, improve thermal cycling resistance, and shorten start-up times. Continued innovation in thin-film electrolytes, interlayers, and perovskite catalysts will be essential for large-scale commercialisation [166].

Lastly, rSOCs face the most complex degradation challenges, including nickel coarsening, electrode delamination, cathode poisoning, and thermomechanical fatigue during frequent mode switching. These are compounded by hydrogen leakage and transient instabilities that complicate grid integration. Research priorities include developing nano-engineered, multifunctional electrodes and stack designs that maintain mechanical and electrochemical stability through repeated thermal cycling at up to  $900 \text{ }^\circ\text{C}$  [167].

Building on these SWOT insights, future research should increasingly link materials innovation with system-level optimisation. The roadmap presented in Fig. 10 integrates these dimensions, showing how progress in materials, control strategies, and deployment frameworks must advance concurrently to accelerate technological readiness. Coordinated progress in durability, manufacturability, and hybrid integration (particularly for rSOC systems) will be critical for their transition from laboratory prototypes to commercially viable, grid-connected technologies.

## 7. Conclusions

SOC technologies represent a versatile and high-efficiency pathway for advancing sustainable energy systems. Their unique ability to operate at high temperatures enables superior fuel flexibility, integration with renewable resources, and the potential for carbon-neutral fuel production and long-duration energy storage. SOECs allow the conversion of electricity into hydrogen or syngas, supporting energy storage and sector coupling, and SOFCs offer efficient power generation. rSOCs, capable of switching between fuel cell and electrolysis modes, provide compelling solutions for grid balancing and seasonal energy storage.

This study has provided a review of the electrochemical principles, recent material innovations, and emerging strategies for SOC technologies. Looking ahead, the future success of high-temperature electrochemical energy conversion depends on continued innovation across several fronts. SOEC technology must scale to multi-megawatt installations while harnessing thermal synergies. SOFC systems must evolve toward lower-temperature operation and expedited startup capabilities. rSOC development requires an integration of materials science developments, stack reliability enhancements, and system-level

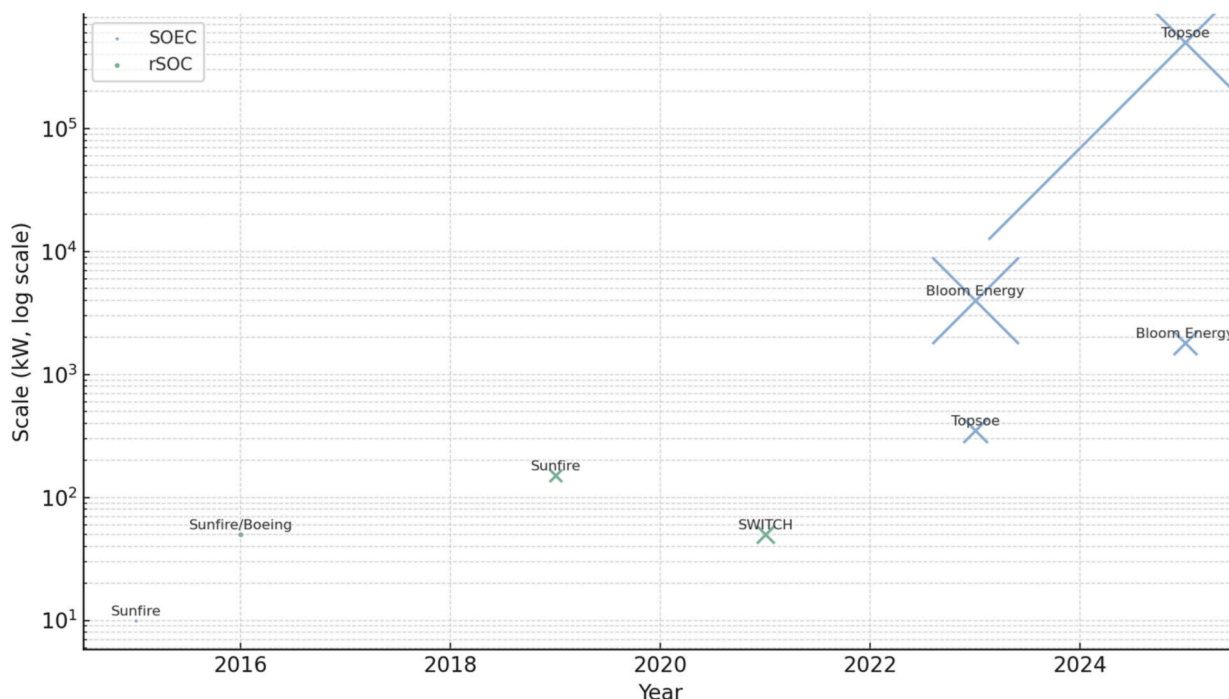


Fig. 8. Global demonstration projects of SOEC and rSOC technologies timeline and scale.



Fig. 9. SWOT analysis of SOFC, SOEC, and rSOC.

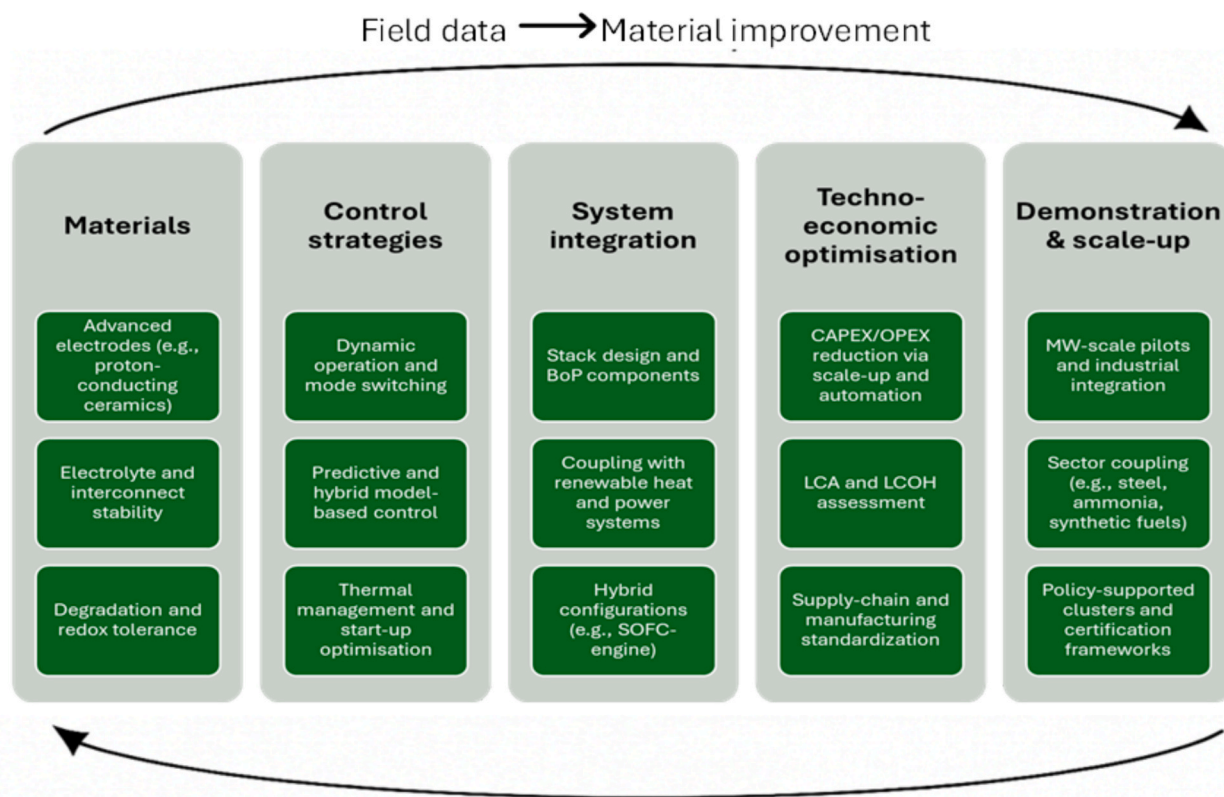


Fig. 10. Roadmap for SOC technology development, linking materials, control, system integration, economics, and demonstration.

control strategies to manage dual-mode operation safely and robustly. In practical terms, SOFCs are particularly well-suited for stationary distributed generation and CHP systems, where their high electrical

efficiency and fuel flexibility can offset installation costs. However, their widespread applicability remains constrained by challenges such as long start-up times, thermal management issues, and degradation under

dynamic operation, which currently limit their use in mobile or rapidly cycling applications. Addressing these limitations through advances in materials, system integration, and cost reduction will be essential to unlock the full commercial potential of SOFC technology.

Given the different maturity levels of SOEC, SOFC, and rSOC technologies, R&D priorities should be differentiated. For SOECs, the focus should be on enhancing stack durability, lowering manufacturing costs, and validating large-scale co-electrolysis for synthetic fuel production. SOFC efforts should target intermediate-temperature operation, improved thermal cycling, and modular designs for distributed generation. Meanwhile, rSOC development should emphasize durable bidirectional electrodes, robust control systems, and integration into hybrid energy storage schemes. This prioritization aligns research progress with realistic deployment timelines.

At a broader level, supportive frameworks that link technological progress with industrial deployment will be essential to accelerate scale-up. Encouraging collaborative demonstration projects, harmonizing performance standards, and fostering partnerships between research and industry can help bridge the gap between innovation and market uptake, ensuring that SOFC technologies advance coherently along their respective readiness pathways.

#### CRedit authorship contribution statement

**Bruna Rijo:** Writing – review & editing, Writing – original draft, Conceptualization. **Cecilia Mateos-Pedrero:** Writing – review & editing, Writing – original draft. **José R. Copa Rey:** Writing – review & editing, Writing – original draft. **Andrei Longo:** Writing – review & editing, Writing – original draft. **Paulo Brito:** Writing – review & editing, Writing – original draft. **Catarina Nobre:** Writing – review & editing, Writing – original draft, Validation.

#### Declaration of competing interest

The authors declare that they have no known competing financial interests or personal relationships that could have appeared to influence the work reported in this paper.

#### Acknowledgements

The authors acknowledge Fundação para a Ciência e a Tecnologia, I. P. (Portuguese Foundation for Science and Technology) under project UIDB/05064/2020 (VALORIZA – Research Center for Endogenous Resource Valorization), and the HYFUELUP project under grant agreement no. 101084148.

#### Data availability

Data will be made available on request.

#### References

- [1] Hauch A, Küngas R, Blennow P, Hansen AB, Hansen JB, Mathiesen B, et al. Recent advances in solid oxide cell technology for electrolysis. *Science* (80) 2020;370. <https://doi.org/10.1126/science.aba6118>.
- [2] Talukdar A, Chakrovorty A, Sarmah P, Paramasivam P, Kumar V, Yadav S, et al. A review on solid oxide fuel cell technology: an efficient energy conversion system. *Int J Energy Res* 2024;2024. <https://doi.org/10.1155/2024/6443247>.
- [3] Qian J, Lin C, Chen Z, Huang J, Ai N, Jiang S, et al. High-performance, stable buffer-layer-free La<sub>0.9</sub>Sr<sub>0.1</sub>Ga<sub>0.8</sub>Mg<sub>0.2</sub>O<sub>3</sub> electrolyte-supported solid oxide cell with a nanostructured nickel-based hydrogen electrode. *Appl Catal B Environ* 2024;346. <https://doi.org/10.1016/j.apcatb.2024.123742>.
- [4] Kim SJ, Choi M, Mun T, Woo D, Lee W. Infiltrated nanofiber-based nanostructured electrodes for solid oxide fuel cells. *Int J Energy Res* 2023;2023:10. <https://doi.org/10.1155/2023/7410245>.
- [5] Helal H, Ahrouch M, Rabehi A, Zappa D, Comini E. Nanostructured materials for enhanced performance of solid oxide fuel cells: a comprehensive review. *Crystals* 2024;14. <https://doi.org/10.3390/cryst14040306>.
- [6] Leng Z, Huang Z, Zhou X, Zhang B, Bai H, Zhou J, et al. The effect of sintering aids on BaCe<sub>0.7</sub>Zr<sub>0.1</sub>Y<sub>0.1</sub>O<sub>3-δ</sub> as the electrolyte of proton-conducting solid oxide electrolysis cells. *Int J Hydrogen Energy* 2022;47. <https://doi.org/10.1016/j.ijhydene.2022.07.237>.
- [7] Bi L, Shafi S, Da'as E, Traversa E. Tailoring the Cathode-Electrolyte Interface with Nanoparticles for Boosting the Solid Oxide Fuel Cell Performance of Chemically Stable Proton-Conducting Electrolytes. *Small* 2018;14. <https://doi.org/10.1002/sml.201801231>.
- [8] Kane N, Luo Z, Zhou Y, Ding Y, Weidenbach A, Zhang W, et al. Durable and High-Performance Thin-Film BHyb-Coated BZCYb Bilayer Electrolytes for Proton-Conducting Reversible Solid Oxide Cells. *ACS Appl Mater Interfaces* 2023;15:32395–403. <https://doi.org/10.1021/acsami.3c04627>.
- [9] Rajendran S, Thangavel NK, Ding H, Ding Y, Ding D, Arava LMR. Tri-Doped BaCe<sub>0.3</sub>BaZr<sub>0.3</sub>O<sub>3</sub> as a Chemically Stable Electrolyte with High Proton-Conductivity for Intermediate Temperature Solid Oxide Electrolysis Cells (SOECs). *ACS Appl Mater Interfaces* 2020;12. <https://doi.org/10.1021/acsami.0c12532>.
- [10] Zhang W, Hu Y. Progress in proton-conducting oxides as electrolytes for low-temperature solid oxide fuel cells: From materials to devices. *Energy Sci Eng* 2021;9:1011–984. <https://doi.org/10.1002/ese3.886>.
- [11] Murphy R, Zhou Y, Zhang L, Soule L, Zhang W, Chen Y, et al. A New Family of Proton-Conducting Electrolytes for Reversible Solid Oxide Cells: BaHf<sub>x</sub>Ce<sub>0.8-x</sub>Y<sub>0.1</sub>Yb<sub>0.1</sub>O<sub>3-δ</sub>. *Adv Funct Mater* 2020;30. <https://doi.org/10.1002/adfm.202002265>.
- [12] Li G, Li C, Li Y, Zou P, Liu J, Li N, et al. Technical analysis of a combined heating and power system based on solid oxide fuel cell for building application. *Mater Sci Eng B* 2025;312. <https://doi.org/10.1016/j.mseb.2024.117871>.
- [13] Gong C, Luo X, Tu Z. Performance evaluation of a solid oxide fuel cell multi-stack combined heat and power system with two power distribution strategies. *Energy Convers Manag* 2022;254. <https://doi.org/10.1016/j.enconman.2022.115302>.
- [14] Sun B, Tian L, Hou J, An Q. Multi-criteria assessment and optimization of a natural gas-fed solid oxide fuel cell combined heat and power system. *Int J Thermofluids* 2023;20. <https://doi.org/10.1016/j.ijft.2023.100420>.
- [15] Wang J, Cui Z, Yao W, Huo S. Regulation strategies and thermodynamic analysis of combined cooling, heating, and power system integrated with biomass gasification and solid oxide fuel cell. *Energy* 2022;266. <https://doi.org/10.1016/j.energy.2022.126430>.
- [16] Lamagna M, Groppi D, Nastasi B. Reversible solid oxide cells applications to the building sector. *Int J Hydrogen Energy* 2023;48. <https://doi.org/10.1016/j.ijhydene.2023.03.387>.
- [17] Golkhatmi SZ, Asghar M, Lund P. A review on solid oxide fuel cell durability: Latest progress, mechanisms, and study tools. *Renew Sustain Energy Rev* 2022;161. <https://doi.org/10.1016/j.rser.2022.112339>.
- [18] Shin J-S, Saqib M, Jo M, Park K, Park K, Ahn J, et al. A review on solid oxide fuel cell durability: Latest progress, mechanisms, and study tools. *ACS Appl Mater Interfaces* 2022;16:1. <https://doi.org/10.1021/acsami.1c13779>.
- [19] Giridhar N, Allan D, Li M, Zitney S, Biegler L, Bhattacharyya D. Optimal operation of solid-oxide electrolysis cells considering long-term chemical degradation. *Energy Convers Manag* 2024;319. <https://doi.org/10.1016/j.enconman.2024.118950>.
- [20] Liu G-Q, Zhou Y, Liu X, Li Z, Kupecki J, Jin B, et al. Multiscale analysis and cost optimization of a reversible solid oxide cell system with coordinated degradation and efficiency considering Ni-particle coarsening. *J Clean Prod* 2023;424. <https://doi.org/10.1016/j.jclepro.2023.138823>.
- [21] Chen K, Jiang S. Review—Materials Degradation of Solid Oxide Electrolysis Cells. *J Electrochem Soc* 2016;163. <https://doi.org/10.1149/2.0101611JES>.
- [22] Yang Y, Lei J, Huang X, Liao Z, Liu Y, Tu Z. Recent development in reversible solid oxide fuel cells: theory, integration and prospective. *ChemElectroChem* 2024;11:e202300593. <https://doi.org/10.1002/celec.202300593>.
- [23] Saarinen V, Pennanen J, Kotisaari M, Thomann O, Himanen O, Di IS, et al. Design, manufacturing, and operation of movable 2 × 10 kW size rSOC system. *Fuel Cells* 2021;21:477–87. <https://doi.org/10.1002/fuce.202100021>.
- [24] Corigliano O, Pagnotta L, Fragiaco P. On the Technology of Solid Oxide Fuel Cell (SOFC) Energy Systems for Stationary Power Generation. A Review. *Sustain* 2022;14. <https://doi.org/10.3390/su142215276>.
- [25] Qiu P, Li C, Liu B, Yan D, Li J, Jia L. Materials of solid oxide electrolysis cells for H<sub>2</sub>O and CO<sub>2</sub> electrolysis: A review. *J Adv Ceram* 2023;12:1463–510. <https://doi.org/10.26599/JAC.2023.9220767>.
- [26] Sadeghzadeh M, Mehrpooya M, Ansarinabab H. A novel exergy-based assessment on a multi-production plant of power, heat and hydrogen: integration of solid oxide fuel cell, solid oxide electrolyzer cell and Rankine steam cycle. *Int J Low-Carbon Technol* 2021;16:798–813. <https://doi.org/10.1093/ijlct/ctab008>.
- [27] Rabet S, Sharafi S, Habibi O, Ali S, Jahanshahi S, Yari M, et al. A novel multi-generation system integrating thermophotovoltaic and SOFC system for power and green hydrogen with CO<sub>2</sub> liquefaction: A techno-economic and multi-objective optimization study. *Fuel* 2026;405:136581. <https://doi.org/10.1016/j.fuel.2025.136581>.
- [28] Sharafi S, Sadat H, Mousavi R, Rabet S, Nojavan F. Solar thermal assisted proton exchange membrane electrolyzer and solid oxide fuel cell system based on biomass gasification for green power and hydrogen production: Multi-objective optimization and exergoeconomic analysis. *Energy Convers Manag* 2025;337:119900. <https://doi.org/10.1016/j.enconman.2025.119900>.
- [29] Liu H, Yu M, Tong X, Wang Q, Chen M. High Temperature Solid Oxide Electrolysis for Green Hydrogen Production. *Chem Rev* 2024;124:10509–76. <https://doi.org/10.1021/acs.chemrev.3c00795>.
- [30] Yoon S-E, Song S-H, Choi J, Ahn J-Y, Kim B-K, Park J-S. Coelectrolysis of steam and CO<sub>2</sub> in a solid oxide electrolysis cell with ceramic composite electrodes. *Int J Hydrogen Energy* 2014;39:5497–504. <https://doi.org/10.1016/j.ijhydene.2014.01.124>.

- [31] Wang J, Wen J, Wang J, Yang B, Jiang L. Water electrolyzer operation scheduling for green hydrogen production: A review. *Renew Sustain Energy Rev* 2024;203:114779. <https://doi.org/10.1016/j.rser.2024.114779>.
- [32] Wang Z, Wang Y, Li N, Tong Y, Teng Y, Wang D, et al. Performance and durability of metal-supported solid oxide electrolysis cells at intermediate temperatures. *Int J Hydrogen Energy* 2023;48:12949–57. <https://doi.org/10.1016/j.ijhydene.2022.12.191>.
- [33] Ruiz Diaz DF, Wang Y. Component-level modeling of solid oxide water electrolysis cell for clean hydrogen production. *J Clean Prod* 2024;443:140940. <https://doi.org/10.1016/j.jclepro.2024.140940>.
- [34] Shiva Kumar S, Lim H. An overview of water electrolysis technologies for green hydrogen production. *Energy Reports* 2022;8:13793–813. <https://doi.org/10.1016/j.egyr.2022.10.127>.
- [35] Flatt RJ, Roussel N, Cheeseman CR. Concrete: An eco material that needs to be improved. *J Eur Ceram Soc* 2012;32:2787–98. <https://doi.org/10.1016/j.jeurceramsoc.2011.11.012>.
- [36] Zhou X, Sun F, Zhang C, Sun C. Stochastically predictive co-optimization of the speed planning and powertrain controls for electric vehicles driving in random traffic environment safely and efficiently. *J Power Sources* 2022;528:231200. <https://doi.org/10.1016/j.jpowsour.2022.231200>.
- [37] Zhang N, Sun J, Sheng J, Yang W, Xue X, Zhang L, et al. Ultrathin chromium oxide buffer layer by reactive thermal deposition for high-performance semitransparent perovskite solar cells. *Mater Today Energy* 2023;35:101338. <https://doi.org/10.1016/j.mtener.2023.101338>.
- [38] Biswas S, Kaur G, Paul G, Giddey S. A critical review on cathode materials for steam electrolysis in solid oxide electrolysis. *Int J Hydrogen Energy* 2023;48:12541–70. <https://doi.org/10.1016/j.ijhydene.2022.11.307>.
- [39] Wang Y, Li W, Ma L, Li W, Liu X. Degradation of solid oxide electrolysis cells: Phenomena, mechanisms, and emerging mitigation strategies—A review. *J Mater Sci Technol* 2020;55:35–55. <https://doi.org/10.1016/j.jmst.2019.07.026>.
- [40] Chatenet M, Pollet BG, Dekel DR, Dionigi F, Deseure J, Millet P, et al. Water electrolysis: from textbook knowledge to the latest scientific strategies and industrial developments. *Chem Soc Rev* 2022;51:4583–762. <https://doi.org/10.1039/D0CS01079K>.
- [41] Schwarze K, Geißler T, Nimitz M, Blumentritt R. Demonstration and scale-up of high-temperature electrolysis systems. *Fuel Cells* 2023;23:492–500. <https://doi.org/10.1002/fuce.202300059>.
- [42] Mitsubishi Heavy Industries. MHI Begins Operation of SOEC Test Module the Next- Generation High-Efficiency Hydrogen Production Technology at Takasago Hydrogen Park - The Path to Higher Output and Greater Capacity - 2024:13–5. <https://www.mhi.com/news/240425.html> (accessed July 21, 2025).
- [43] Voltachem. Collaboration between TNO and Elcogen to develop advanced Solid Oxide Electrolyser Technology 2024:1–10. <https://www.voltachem.com/news/collaboration-between-tno-and-elcogen-to-develop-advanced-solid-oxide-electrolyser-technology> (accessed July 21, 2025).
- [44] Elcogen. Elcogen and Convia celebrate a key development milestone in green hydrogen production technology 2024. <https://elcogen.com/elcogen-and-convia-celebrate-a-key-development-milestone-in-green-hydrogen-production-technology/> (accessed July 21, 2025).
- [45] Fraunhofer IKTS. Thyssenkrupp nucera and Fraunhofer IKTS open First SOEC Pilot Production Plant for Stacks for the Production of Green Hydrogen. 2025.
- [46] SYRIUS project. The European Commission awards the SYRIUS project: A step forward for hydrogen in steelmaking 2025:3.
- [47] SYRIUS Project. Integrating a SOE producing green hydrogen in real steel manufacturing plant to reduce CO2 emissions 2025:8.
- [48] Hydrogen Europe. Consortium unveils 85% -Efficient solid oxide electrolyser. 2024.
- [49] Mbatha S, Cui X, Panah PG, Thomas S, Parkhomenko K, Roger A-C, et al. Comparative evaluation of the power-to-methanol process configurations and assessment of process flexibility. *Energy Adv* 2024;3:2245–70. <https://doi.org/10.1039/D4YA00433G>.
- [50] Offshore-Energy. EnBW markets green ammonia from SkiGA project in Norway. 2024.
- [51] GMK Center. Morocco approves green hydrogen projects worth \$ 32.5 billion. 2025.
- [52] Nasser M, Hassan H. Assessment of hydrogen production from waste heat using hybrid systems of Rankine cycle with proton exchange membrane/solid oxide electrolyzer. *Int J Hydrogen Energy* 2023;48:7135–53. <https://doi.org/10.1016/j.ijhydene.2022.11.187>.
- [53] El-Shafie M. Hydrogen production by water electrolysis technologies: A review. *Results Eng* 2023;20:101426. <https://doi.org/10.1016/j.rineng.2023.101426>.
- [54] Zainal BS, Ker PJ, Mohamed H, Ong HC, Fattah IMR, Rahman SMA, et al. Recent advancement and assessment of green hydrogen production technologies. *Renew Sustain Energy Rev* 2024;189:113941. <https://doi.org/10.1016/j.rser.2023.113941>.
- [55] Nnabuife SG, Hamzat AK, Whidborne J, Kuang B, Jenkins KW. Integration of renewable energy sources in tandem with electrolysis: A technology review for green hydrogen production. *Int J Hydrogen Energy* 2025;107:218–40. <https://doi.org/10.1016/j.ijhydene.2024.06.342>.
- [56] Akyüz ES, Tellî E, Farsak M. Hydrogen generation electrolyzers: Paving the way for sustainable energy. *Int J Hydrogen Energy* 2024;81:1338–62. <https://doi.org/10.1016/j.ijhydene.2024.07.175>.
- [57] Syaqui A, Nagulapati VM, Chaniago YD, Ningtyas JA, Andika R, Lim H. Advancement in power-to-methanol integration with steel industry waste gas utilization through solid oxide electrolyzer cells: Surrogate model-based approach for optimization. *Sustain Energy Technol Assessments* 2025;73:104160. <https://doi.org/10.1016/j.seta.2024.104160>.
- [58] Fogel S, Unger S, Hampel U. Dynamic system modeling and simulation of a power-to-methanol process based on proton-conducting tubular solid oxide cells. *Energy Convers Manag* 2024;300:117970. <https://doi.org/10.1016/j.enconman.2023.117970>.
- [59] Banu A, Bicer Y. Energy and exergy analysis of an integrated system with solar methane cracking and co-electrolysis of CO<sub>2</sub>/H<sub>2</sub>O for efficient carbon management. *Int J Hydrogen Energy* 2024;52:580–93. <https://doi.org/10.1016/j.ijhydene.2023.09.163>.
- [60] Ostadi M, Bromberg L, Cohn DR, Gençer E. Flexible methanol production process using biomass/municipal solid waste and hydrogen produced by electrolysis and natural gas pyrolysis. *Fuel* 2023;334:126697. <https://doi.org/10.1016/j.fuel.2022.126697>.
- [61] Detchusanarand T, Wiranarongkorn K, Im-orb K. Techno-economic performance analysis of biomass-to-methanol with solid oxide electrolyzer for sustainable bio-methanol production. *Energy* 2024;313:133764. <https://doi.org/10.1016/j.energy.2024.133764>.
- [62] Emadi M, Barahimi V, Croiset E. Integrated direct air CO<sub>2</sub> capture and solid oxide electrolyzer for sustainable chemical production: Case studies of methanol and synthesis fuel. *J CO<sub>2</sub> Util* 2025;96:103096. <https://doi.org/10.1016/j.jcou.2025.103096>.
- [63] Park J, Qi M, Baek J, Choi D, Kwon EE, Cho H, et al. Bio-e-methanol production via biogas partial oxidation integrated with solid oxide electrolyzer cell: A comprehensive energy, exergy, economic, and environmental (4E) analysis. *Energy Convers Manag* 2025;341:120052. <https://doi.org/10.1016/j.enconman.2025.120052>.
- [64] Abousalmia A, Al-Remaihi L, Al-Kaabi S, Jassim F, Karagoz S. Simulation and Environmental Sustainability Assessment of an Integrated LNG-Power Cycle-Electrolyzer-Methanol Process for Clean Energy Generation. *Processes* 2025;13. <https://doi.org/10.3390/pr13051476>.
- [65] Lee JM, Lee S, Kye DH, Park HJ, Park W, Shin J, et al. Environ-economic analysis of high-temperature steam electrolysis for decentralized hydrogen production. *Energy Convers Manag* 2022;266:115856. <https://doi.org/10.1016/j.enconman.2022.115856>.
- [66] Fei Z, Zhanguo SU, Lu J, Singh PK, Dahari M, Majidi HS, et al. Sustainable H<sub>2</sub> production/separation by integration of solid oxide electrolyzer, biomass gasifier and H<sub>2</sub> separation membrane: A techno-economic/environmental evaluation and multi-objective optimization. *Process Saf Environ Prot* 2023;177:909–20. <https://doi.org/10.1016/j.psep.2023.07.047>.
- [67] Lim D, Lee B, Lee H, Byun M, Lim H. Projected cost analysis of hybrid methanol production from tri-reforming of methane integrated with various water electrolysis systems: Technical and economic assessment. *Renew Sustain Energy Rev* 2022;155:111876. <https://doi.org/10.1016/j.rser.2021.111876>.
- [68] Nami H, Hendriksen PV, Frandsen HL. Green ammonia production using current and emerging electrolysis technologies. *Renew Sustain Energy Rev* 2024;199:114517. <https://doi.org/10.1016/j.rser.2024.114517>.
- [69] Bui T, Lee D, Ahn KY, Kim YS. Techno-economic analysis of high-power solid oxide electrolysis cell system. *Energy Convers Manag* 2023;278:116704. <https://doi.org/10.1016/j.enconman.2023.116704>.
- [70] Cavalcanti EJC, Rufino CTF, Lima AAS, Azevedo JLB. Model, energy and economic analyses of solid oxide electrolysis cells for clean hydrogen production. *Renew Energy* 2025;254:123747. <https://doi.org/10.1016/j.renene.2025.123747>.
- [71] Jiménez-Martín G, Judez X, Aguado M, Garbayo I. Techno-economic assessment of MW-scale solid oxide electrolysis hydrogen production plant: Integrating possibilities in Spain. *Int J Hydrogen Energy* 2025;142:627–41. <https://doi.org/10.1016/j.ijhydene.2024.12.239>.
- [72] Zhang H, Desideri U. Techno-economic optimization of power-to-methanol with co-electrolysis of CO<sub>2</sub> and H<sub>2</sub>O in solid-oxide electrolyzers. *Energy* 2020;199:117498. <https://doi.org/10.1016/j.energy.2020.117498>.
- [73] Yousaf M, Mahmood A, Elkamel A, Rizwan M, Zaman M. Techno-economic analysis of integrated hydrogen and methanol production process by CO<sub>2</sub> hydrogenation. *Int J Greenh Gas Control* 2022;115:103615. <https://doi.org/10.1016/j.ijggc.2022.103615>.
- [74] Khan MHA, Sitaraman T, Haque N, Leslie G, Saydam S, Daiyan R, et al. Strategies for life cycle impact reduction of green hydrogen production – Influence of electrolyser value chain design. *Int J Hydrogen Energy* 2024;62:769–82. <https://doi.org/10.1016/j.ijhydene.2024.01.081>.
- [75] *Global Hydrogen Review 2024*. 2024..
- [76] Prosser JH, James BD, Murphy BM, Wendt DS, Casteel MJ, Westover TL, et al. Cost analysis of hydrogen production by high-temperature solid oxide electrolysis. *Int J Hydrogen Energy* 2024;49:207–27. <https://doi.org/10.1016/j.ijhydene.2023.07.084>.
- [77] Liu H, Clausen LR, Wang L, Chen M. Pathway toward cost-effective green hydrogen production by solid oxide electrolyzer. *Energy Environ Sci* 2023;16:2090–111. <https://doi.org/10.1039/D3EE00232B>.
- [78] Freire Ordóñez D, Ganzer C, Halfdanarson T, González Garay A, Patrizio P, Bardow A, et al. Quantifying global costs of reliable green hydrogen. *Energy Adv* 2023;2:2042–54. <https://doi.org/10.1039/D3YA000318C>.
- [79] Li Z, Huang Q, Yang L, Huang H, Wei K, Li D, et al. Energy analysis of hydrogen production via fuel-assisted high-temperature solid oxide electrolysis cell via system modelling. *Sustain Energy Res* 2025;12. <https://doi.org/10.1186/s40807-025-00158-y>.
- [80] Clean Hydrogen Mission. accessed August 1, 2025 *Hydrogen Valleys 2024:6–11*. [https://www.clean-hydrogen.europa.eu/get-involved/hydrogen-valleys\\_en](https://www.clean-hydrogen.europa.eu/get-involved/hydrogen-valleys_en).

- [81] Zarabi Golkhatmi S, Asghar MI, Lund PD. A review on solid oxide fuel cell durability: Latest progress, mechanisms, and study tools. *Renew Sustain Energy Rev* 2022;161:112339. <https://doi.org/10.1016/j.rser.2022.112339>.
- [82] Wei X, Sharma S, Waeber A, Wen D, Margni M, Maréchal F, et al. Environmental implications of solid oxide fuel cell system for hydrogen sustainability. *Resour Conserv Recycl* 2025;215:108134. <https://doi.org/10.1016/j.resconrec.2025.108134>.
- [83] Wei X, Sharma S, Waeber A, Van Herle J, Maréchal F. Integrated Solid Oxide Systems: Advancing Efficiency in Power Generation through Fuel Cell-Electrolyzer Coupling with Diverse Fuels. *Comput Aided Chem Eng* 2024;53: 979–84. <https://doi.org/10.1016/B978-0-443-28824-1.50164-2>.
- [84] Yattoo MA, Habib F, Malik AH, Qazi MJ, Ahmad S, Ganayee MA, et al. Solid-oxide fuel cells: A critical review of materials for cell components. *MRS Commun* 2023; 13:378–84. <https://doi.org/10.1557/s43579-023-00371-0>.
- [85] Yang F, Jia L, Zhou Y, Guan D, Feng K, Choi Y, et al. Life cycle assessment shows that retrofitting coal-fired power plants with fuel cells will substantially reduce greenhouse gas emissions. *One Earth* 2022;5:392–402. <https://doi.org/10.1016/J.ONEEAR.2022.03.009>.
- [86] Hao Q, Zhu L, Fan J, Wang Y, Yang Z, Yang H, et al. Zero-energy penalty carbon capture and utilization system based on CLHG integrating SOFC for power and methanol cogeneration. *Energy Convers Manag* 2023;295:117658. <https://doi.org/10.1016/j.enconman.2023.117658>.
- [87] Bhoga SS, Khandale AP. Cathode materials for intermediate temperature solid oxide fuel cells. *Indian J Pure Appl Phys* 2013;51:305–9. <https://doi.org/10.3390/fuels5040045>.
- [88] Vinchhi P, Khandla M, Chaudhary K, Pati R. Recent advances on electrolyte materials for SOFC: A review. *Inorg Chem Commun* 2023;152:110724. <https://doi.org/10.1016/j.inoche.2023.110724>.
- [89] Peng X, Tian Y, Liu Y, Wang W, Jing chen, Li J, et al. A double perovskite decorated carbon-tolerant redox electrode for symmetrical SOFC. *Int J Hydrogen Energy* 2020;45:14461–9. <https://doi.org/10.1016/j.ijhydene.2020.03.151>.
- [90] Liu Y, Luo J, Li C, Liu B, Yan D, Li J, et al. BaCe<sub>0.8</sub>Fe<sub>0.1</sub>Ni<sub>0.1</sub>O<sub>3-δ</sub>-impregnated Ni-GDC by phase-inversion as an anode of solid oxide fuel cells with on-cell dry methane reforming. *J Adv Ceram* 2024;13:834–41. <https://doi.org/10.26599/JAC.2024.9220902>.
- [91] R. Scatagliini, M. Wei, A. Mayyas, S. H. Chan, T. Lipman MS. A Direct Manufacturing Cost Model for Solid-Oxide Fuel Cell Stacks 2017;17. Doi: 10.1002/fuce.201700012.
- [92] International Energy Agency I. The Future of Hydrogen. 2019. Doi: 10.1787/1e0514c4-en.
- [93] Ahmad MZ, Ahmad SH, Chen RS, Ismail AF, Hazan R, Baharuddin NA. Review on recent advancement in cathode material for lower and intermediate temperature solid oxide fuel cells application. *Int J Hydrogen Energy* 2022;47:1103–20. <https://doi.org/10.1016/J.IJHYDENE.2021.10.094>.
- [94] Iea. *The Future of Hydrogen. Seizing today's opportunities*. 2019.
- [95] Clean Hydrogen Joint Undertaking. Strategic Research and Innovation Agenda 2021–2027. 2013. Doi: 10.13140/2.1.4252.7520.
- [96] Uecker J, Unachukwu ID, Vibhu V, Vinke IC, Eichel RA, (Bert) de Haart LGJ. Performance, electrochemical process analysis and degradation of gadolinium doped ceria as fuel electrode material for solid oxide electrolysis cells. *Electrochim Acta* 2023;452:142320. <https://doi.org/10.1016/J.ELECTACTA.2023.142320>.
- [97] Li M, Hua B, Luo J, Jiang SP, Pu J, Chi B, et al. Enhancing Sulfur Tolerance of Ni-Based Cermet Anodes of Solid Oxide Fuel Cells by Ytterbium-Doped Barium Cerate Infiltration. *ACS Appl Mater & Interfaces* 2016;8:10293–301. <https://doi.org/10.1021/acsami.6b00925>.
- [98] Pirkandi J, Ommian M. Thermo-Economic Operation Analysis of SOFC-GT Combined Hybrid System for Application in Power Generation Systems. *J Electrochem Energy Convers Storage* 2018;16. <https://doi.org/10.1115/1.4400056>.
- [99] Yadav AK, Sinha S, Kumar A. Advancements in composite cathodes for intermediate-temperature solid oxide fuel cells: A comprehensive review. *Int J Hydrogen Energy* 2024;59:1080–93. <https://doi.org/10.1016/J.IJHYDENE.2024.02.124>.
- [100] Marocco P, Gandiglio M, Santarelli M. When SOFC-based cogeneration systems become convenient? A cost-optimal analysis. *Energy Reports* 2022;8:8709–21. <https://doi.org/10.1016/j.egy.2022.06.015>.
- [101] Gao FY, Gao MR. Nickel-Based Anode Catalysts for Efficient and Affordable Anion-Exchange Membrane Fuel Cells. *Acc Chem Res* 2023;56:1445–57. <https://doi.org/10.1021/acs.accounts.3c00071>.
- [102] Piccardo P, Spotorno R, Geipel C. Investigation of a Metallic Interconnect Extracted from an SOFC Stack after 40,000 h of Operation. *Energies* 2022;15. <https://doi.org/10.3390/en15103548>.
- [103] Yang S, Gao J, Trini M, De Angelis S, Jørgensen PS, Bowen JR, et al. Ni coarsening in Ni-yttria stabilized zirconia electrodes: Three-dimensional quantitative phase-field simulations supported by ex-situ ptychographic nano-tomography. *Acta Mater* 2023;246:118708. <https://doi.org/10.1016/j.actamat.2023.118708>.
- [104] Li B, He S, Li J, Yue X, Irvine JTS, Xie D, et al. A Ce/Ru Codoped SrFeO<sub>3-δ</sub> Perovskite for a Coke-Resistant Anode of a Symmetrical Solid Oxide Fuel Cell. *ACS Catal* 2020;10:14398–409. <https://doi.org/10.1021/acscatal.0c03554>.
- [105] Fan Y, Xi X, Li J, Wang Q, Xiang K, Medvedev D, et al. Barium-doped Sr<sub>2</sub>Fe<sub>1.5</sub>Mo<sub>0.5</sub>O<sub>6-δ</sub> perovskite anode materials for protonic ceramic fuel cells for ethane conversion. *J Am Ceram Soc* 2022;105:3613–24. <https://doi.org/10.1111/jace.18329>.
- [106] Zhang S, Wan Y, Xu Z, Xue S, Zhang L, Zhang B, et al. Bismuth doped La<sub>0.75</sub>Sr<sub>0.25</sub>Cr<sub>0.5</sub>Mn<sub>0.5</sub>O<sub>3-δ</sub> perovskite as a novel redox-stable efficient anode for solid oxide fuel cells. *J Mater Chem A* 2020;8:11553–63. <https://doi.org/10.1039/D0TA03328F>.
- [107] Zainon AN, Baharuddin NA, Lim BH, Wan Yusoff WNA, Wan Abdullah WS, Raharjo J. Biofuels in solid oxide fuel cell systems: a review of production, applications, challenges, and future prospects. *Fuel* 2026;406:137092. <https://doi.org/10.1016/j.fuel.2025.137092>.
- [108] Antolini E. Molten Metals and Molten Carbonates in Solid Oxide Direct Carbon Fuel Cell Anode Chamber: Liquid Metal Anode and Hybrid Direct Carbon Fuel Cells. *Catalysts* 2023;13. <https://doi.org/10.3390/catal13071107>.
- [109] Jayakumar A, Küngas R, Roy S, Javadekar A, Buttrey DJ, Vohs JM, et al. A direct carbon fuel cell with a molten antimony anode. *Energy Environ Sci* 2011;4: 4133–7. <https://doi.org/10.1039/C1EE01863A>.
- [110] Liu B, Li Q, Ke Y, Li G, Yan D, Li J, et al. Review on the application of PdO/Pd in cathode modification for solid oxide fuel cells. *Int J Hydrogen Energy* 2025;106: 586–603. <https://doi.org/10.1016/j.ijhydene.2025.01.501>.
- [111] Li H, Wang W, Lin J, Park K-Y, Lee T, Heyden A, et al. Improved cell performance and sulphur tolerance using A-site substituted Sr<sub>2</sub>Fe<sub>1.4</sub>Ni<sub>0.1</sub>Mo<sub>0.5</sub>O<sub>6-δ</sub> anodes for solid-oxide fuel cells. *Clean Energy* 2023;7:70–83. <https://doi.org/10.1093/ce/zkac089>.
- [112] Rahumi O, Yuferov Y, Meshi L, Maman N, Borodianskiy K. Ni-doping strategy for perovskite anodes towards high-performance ammonia-fueled SOFCs. *J Power Sources* 2025;631:236320. <https://doi.org/10.1016/j.jpowsour.2025.236320>.
- [113] Yang Y, Lei J, Huang X, Liao Z, Liu Y, Tu Z. Recent Development in Reversible Solid Oxide Fuel Cells: Theory, Integration and Prospective. *ChemElectroChem* 2024;11. <https://doi.org/10.1002/celec.202300593>.
- [114] Venkataraman V, Pérez-Fortes M, Wang L, Hajimolana YS, Boigues-Muñoz C, Agostini A, et al. Reversible solid oxide systems for energy and chemical applications – Review & perspectives. *J Energy Storage* 2019;24:100782. <https://doi.org/10.1016/j.est.2019.100782>.
- [115] Loboichenko V, Casado-Manzano M, Navas SJ, Toharias B, Rosa F, Iranzo A. Ammonia as energy source for solid oxide fuel cell technology. *Energy Reports* 2025;13:5828–47. <https://doi.org/10.1016/j.egy.2025.05.020>.
- [116] Banasiak D, Gallaun M, Rinnhofer C, Kienberger T. Integration of a rSOC-system to industrial processes. *Energy Convers Manag X* 2023;20:100425. <https://doi.org/10.1016/j.ecmx.2023.100425>.
- [117] Yang C, Jing X, Miao H, Xu J, Lin P, Li P, et al. The physical properties and effects of sintering conditions on rSOC fuel electrodes evaluated by molecular dynamics simulation. *Energy* 2021;216:119215. <https://doi.org/10.1016/j.energy.2020.119215>.
- [118] Xu Y, Cai S, Chi B, Tu Z. Technological limitations and recent developments in a solid oxide electrolyzer cell: A review. *Int J Hydrogen Energy* 2024;50:548–91. <https://doi.org/10.1016/j.ijhydene.2023.08.314>.
- [119] Posdziech O, Schwarze K, Brabandt J. Efficient hydrogen production for industry and electricity storage via high-temperature electrolysis. *Int J Hydrogen Energy* 2019;44:19089–101. <https://doi.org/10.1016/j.ijhydene.2018.05.169>.
- [120] Parashar A, Vaeth A, Rizvandi OB, Swartz SL, Braun RJ. Performance analysis of a 1 MW reversible solid oxide system for flexible hydrogen and electricity production. *Int J Hydrogen Energy* 2025;101:1116–35. <https://doi.org/10.1016/j.ijhydene.2024.12.320>.
- [121] Liang Y, Wang J, Ling X, Zhu Y, Yao S. Energy, exergy and economic (3E) analysis of a novel hydrogen storage/power generation system based on a reversible solid oxide fuel cell. *Renew Energy* 2025;253:123643. <https://doi.org/10.1016/j.renene.2025.123643>.
- [122] Martsinchyk A, Milewski J, Szczesniak A, Dybinski O, Shuhayev P, Sienko A, et al. Operation of solid oxide fuel cell stack in reversible mode for hydrogen generation for molten carbonate fuel cell as power-to-gas process. *Chem Eng J* 2025;507:160624. <https://doi.org/10.1016/j.cej.2025.160624>.
- [123] Wang H, Lei Z, Sang J, Wang X, Li J, Yang Z, et al. One-pot molten salt synthesis of Ce<sub>0.9</sub>Gd<sub>0.1</sub>O<sub>2-δ</sub>@PrBa<sub>0.5</sub>Sr<sub>0.5</sub>Co<sub>2</sub>O<sub>5+δ</sub> as the oxygen electrode for reversible solid oxide cells. *Mater Res Bull* 2023;160:112115. <https://doi.org/10.1016/j.materresbull.2022.112115>.
- [124] Rehman SU, Qamar S, Hassan MH, Kim H-S, Song R-H, Lim T-H, et al. Exceptionally stable nanostructured air electrodes for reversible solid oxide fuel cells via crystallization-assisted infiltration. *J Eur Ceram Soc* 2023;43:1559–66. <https://doi.org/10.1016/j.jeurceramsoc.2022.11.041>.
- [125] Yang C, Guo R, Jing X, Li P, Yuan J, Wu Y. Degradation mechanism and modeling study on reversible solid oxide cell in dual-mode — A review. *Int J Hydrogen Energy* 2022;47:37895–928. <https://doi.org/10.1016/j.ijhydene.2022.08.240>.
- [126] Tian Y, Liu Y, Wang W, Jia L, Pu J, Chi B, et al. High performance and stability of double perovskite-type oxide NdBa<sub>0.5</sub>Ca<sub>0.5</sub>Co<sub>1.5</sub>Fe<sub>0.5</sub>O<sub>5+δ</sub> as an oxygen electrode for reversible solid oxide electrochemical cell. *J Energy Chem* 2020;43:108–15. <https://doi.org/10.1016/j.jechem.2019.08.010>.
- [127] Kwon Y, Kang S, Bae J. Development of a PrBaMn<sub>2</sub>O<sub>5+δ</sub>-La<sub>0.8</sub>Sr<sub>0.2</sub>Ga<sub>0.85</sub>Mg<sub>0.15</sub>O<sub>3-δ</sub> composite electrode by scaffold infiltration for reversible solid oxide fuel cell applications. *Int J Hydrogen Energy* 2020;45: 1748–58. <https://doi.org/10.1016/j.ijhydene.2019.11.054>.
- [128] Lee SW, Lee SH, Park JH, Duan C, Irvine JTS, Shin TH. Reversible solid oxide electrochemical cells with regulated oxygen trapping nano-dots on Ni-Fe fuel electrode. *Chem Eng J* 2025;503:158483. <https://doi.org/10.1016/j.cej.2024.158483>.
- [129] Liu G, Wang Z, Liu X, Kupecki J, Zhao D, Jin B, et al. Transient analysis and safety-oriented process optimization during electrolysis–fuel cell transition of a novel reversible solid oxide cell system. *J Clean Prod* 2023;425:139000. <https://doi.org/10.1016/j.jclepro.2023.139000>.

- [130] Xu Y, Yin J, Wang J, Wu X, Peng J, Tang R, et al. Thermal constraint control of reversible solid oxide cell for optimal system efficiency. *Int J Hydrogen Energy* 2025;134:198–211. <https://doi.org/10.1016/j.ijhydene.2025.04.474>.
- [131] Califano M, Sorrentino M, Pianese C. Energy management control strategies addressing the rSOC degradation phenomena in a polygeneration microgrid. *Int J Hydrogen Energy* 2024;95:1137–50. <https://doi.org/10.1016/j.ijhydene.2024.03.339>.
- [132] Topsoe. Topsoe reaches new milestone: SOEC demo reveals strong results. Topsoe 2024;1–10. <https://www.topsoe.com/blog/breakthrough-in-green-hydrogen-topsoes-soec-demo-reveals-strong-results> (accessed July 22, 2025).
- [133] Hydrogen TechWorld. accessed July 22, 2025 World's largest solid oxide electrolyzer begins producing hydrogen 2023:1–7. <https://hydrogentechworld.com/worlds-largest-solid-oxide-electrolyzer-begins-producing-hydrogen>.
- [134] Riedel M, Heddrich M, Friedrich K. Performance and Durability of a 10 layer SOE Stack operated under pressurized conditions. *Conf. 12th Eur. Fuel Cell Forum*, vol. 475, 2018.
- [135] Riedel M, Heddrich M, Friedrich K. Analysis of pressurized operation of 10 layer solid oxide electrolysis stacks. *Int J Hydrogen Energy* 2019;44. <https://doi.org/10.1016/J.IJHYDENE.2018.12.168>.
- [136] Topsoe. Welcome to Haldor-Topsoe's Vej 2, Home of the EU's largest industrial-scale SOEC manufacturing facility 2025:1–19. <https://www.topsoe.com/herning> (accessed July 22, 2025).
- [137] Energy B. Bloom Energy. accessed July 22, 2025 SK ecoplant to Deploy Electrolyzers for Hydrogen Demonstration 2024:1–4. <https://www.turbomachinery.com/view/bloom-energy-sk-ecoplant-to-deploy-electrolyzers-for-hydrogen-demonstration>.
- [138] Lymeropoulos N, Tsimis D, Aguiló-Rullan A, Atanasio M, Zafeiratou E, Dirmiki D. The Status of SOFC and SOEC R&D in the European Fuel Cell and Hydrogen Joint Undertaking Programme. *ECS Trans* 2019;91. <https://doi.org/10.1149/09101.0009ecst>.
- [139] DGE European Programs. LIFE 2021–2027: EU funding opportunities for the Clean Energy Transition (Climate). 2024. Doi: 10.4324/9781315585055-4.
- [140] Elcogen. Elcogen is awarded for EU Innovation Fund to advance green hydrogen production in Europe 2024. <https://elcogen.com/elcogen-awarded-funding-to-help-eu-develop-affordable-green-hydrogen-technology/> (accessed July 24, 2025).
- [141] Elcogen. Elcogen awarded funding to help EU develop affordable green hydrogen technology 2023:1–9. <https://elcogen.com/elcogen-awarded-funding-to-help-eu-develop-affordable-green-hydrogen-technology/> (accessed July 24, 2025).
- [142] David Garcia Arrate. Driving the EU's Green Transition: Innovation Fund Launches New Calls for Proposals. accessed July 24, 2025 Euro Funding 2025: 1–10. <https://euro-funding.com/en/blog/driving-the-eus-green-transition/>.
- [143] Cheng T, Jiang J, Wu X, Li X, Xu M, Deng Z, et al. Application oriented multiple-objective optimization, analysis and comparison of solid oxide fuel cell systems with different configurations. *Appl Energy* 2019;235:914–29. <https://doi.org/10.1016/j.apenergy.2018.11.038>.
- [144] Casanova A. A consortium approach to commercialized Westinghouse solid oxide fuel cell technology. *J Power Sources* 1998;71:65–70. [https://doi.org/10.1016/S0378-7753\(97\)02757-2](https://doi.org/10.1016/S0378-7753(97)02757-2).
- [145] He V, Gaffuri M, Van herle J, Schiffmann J. Readiness evaluation of SOFC-MGT hybrid systems with carbon capture for distributed combined heat and power. *Energy Convers Manag* 2023;278:116728. <https://doi.org/10.1016/j.enconman.2023.116728>.
- [146] *ECS Trans* 2011;35:113. <https://doi.org/10.1149/1.3569985>.
- [147] EBZ Entwicklungs- und Vertriebsgesellschaft Brennstoffzelle mbH. Data sheet - Fuel Cells SOFC Demonstration Units 2025. [https://download.ebz-dresden.de/images/stories/pdf\\_en/EBZ\\_Fuel\\_Cells\\_Demonstration.pdf](https://download.ebz-dresden.de/images/stories/pdf_en/EBZ_Fuel_Cells_Demonstration.pdf) (accessed July 23, 2025).
- [148] Frenzel I, Loukou A, Trimis D, Schroeter F, Mir L, Marin R, et al. Development of an SOFC based Micro-CHP System in the Framework of the European Project FC-DISTRICT. *Energy Procedia* 2012;28:170–81. <https://doi.org/10.1016/j.egypro.2012.08.051>.
- [149] Rechberger J, Kaupert A, Hagerskans J, Blum L. Demonstration of the First European SOFC APU on a Heavy Duty Truck. *Transp Res Procedia* 2016;14: 3676–85. <https://doi.org/10.1016/j.trpro.2016.05.442>.
- [150] Nabavi SA, Erans M, Manović V. Demonstration of a kW-scale solid oxide fuel cell-calciner for power generation and production of calcined materials. *Appl Energy* 2019;255:113731. <https://doi.org/10.1016/j.apenergy.2019.113731>.
- [151] Kim YS, Lee YD, Ahn KY. System integration and proof-of-concept test results of SOFC-engine hybrid power generation system. *Appl Energy* 2020;277:115542. <https://doi.org/10.1016/j.apenergy.2020.115542>.
- [152] Gandiglio M, Lanzini A, Santarelli M, Aciri M, Hakala T, Rautanen M. Results from an industrial size biogas-fed SOFC plant (the DEMOSOFc project). *Int J Hydrogen Energy* 2020;45:5449–64. <https://doi.org/10.1016/j.ijhydene.2019.08.022>.
- [153] Distel MM, Margutti JM, Obermeier J, Nuß A, Baumeister I, Hritsyshyna M, et al. Large-Scale H<sub>2</sub> Storage and Transport with Liquid Organic Hydrogen Carrier Technology: Insights into Current Project Developments and the Future Outlook. *Energy Technol* 2025;13. <https://doi.org/10.1002/ente.202301042>.
- [154] Herzinger E, Wolf M. Perspectives and Potential of Liquid Organic Hydrogen Carriers in the German Energy Scenario. *Chemie-Ingenieur-Technik* 2024;96: 65–73. <https://doi.org/10.1002/cite.202300227>.
- [155] NETL. New Solid Oxide Fuel Cell System Installed for Demonstration Tests at NETL 2024:23–5. <https://netl.doe.gov/node/14335> (accessed July 23, 2025).
- [156] Skidmore Z. Bloom Energy secures 1GW fuel cell supply deal with AEP. accessed July 23, 2025 Energy Sustain Channel 2025:1–6. <https://www.datacenterdynamics.com/en/news/bloom-energy-secures-1gw-fuel-cell-supply-deal-with-aep/>.
- [157] Dan Y, Wang G, Teketel BS, Beshiwork BA, Liu H, Hanif MB, et al. Empowering Reversible Solid Oxide Cells at the Hydrogen-Electricity Nexus. *Appl Catal B Environ Energy* 2025;362:124677. <https://doi.org/10.1016/j.apcatb.2024.124677>.
- [158] Switch EU Project Consortium. Smart Ways for In-Situ Totally Integrated and Continuous Multisource Generation of Hydroge. 2024.
- [159] Reznicek EP, Braun RJ. Reversible solid oxide cell systems for integration with natural gas pipeline and carbon capture infrastructure for grid energy management. *Appl Energy* 2020;259:114118. <https://doi.org/10.1016/j.apenergy.2019.114118>.
- [160] Perna A, Minutillo M, Jannelli E. Designing and analyzing an electric energy storage system based on reversible solid oxide cells. *Energy Convers Manag* 2018; 159:381–95. <https://doi.org/10.1016/j.enconman.2017.12.082>.
- [161] Fan Y, Chen Y, Abernathy H, Pineault R, Addis R, Song X, et al. Enabling durable hydrogen production and preventing the catastrophic delamination in the solid oxide electrolysis cells by infiltrating SrFe<sub>2</sub>O<sub>4-8</sub> solutions into LSM/YSZ-based air electrode. *J Power Sources* 2023;580:233389. <https://doi.org/10.1016/j.jpowsour.2023.233389>.
- [162] Dong Y, Chen I-W. Inversion of oxygen potential transitions at grain boundaries of SOFC/SOEC electrolytes 2018;1.
- [163] Han F, Lang M, Szabo P, Geipel C, Walter C. Performance and Degradation of Electrolyte Supported SOECs with Advanced Thin-Film Gadolinium Doped Ceria Barrier Layers in Long-Term Stack Test Performance and Degradation of Electrolyte Supported SOECs with Advanced Thin-Film Gadolinium Doped Ceria Bar. *Electrochem Soc* 2024;171:8. <https://doi.org/10.1149/1945-7111/ad4781>.
- [164] Zhang Y, Wen Y, Huang K, Nicholas JD. Atomic Layer Deposited Zirconia Overcoats as On-Board Strontium Getters for Improved Solid Oxide Fuel Cell Nanocomposite Cathode Durability. *ACS Appl Energy Mater* 2020;3:4057–67. <https://doi.org/10.1021/acsaem.0c00558>.
- [165] Machado M, Baiutti F, Bernadet L, Morata A, Nuñez M, Ouweltjes JP, et al. Functional thin films as cathode/electrolyte interlayers: a strategy to enhance the performance and durability of solid oxide fuel cells. *J Mater Chem A* 2022;10: 17317–25. <https://doi.org/10.1039/D2TA03641J>.
- [166] Zhai S, Xie H, Cui P, Guan D, Wang J, Zhao S, et al. A combined ionic Lewis acid descriptor and machine-learning approach to prediction of efficient oxygen reduction electrodes for ceramic fuel cells. *Nat Energy* 2022;7:866–75. <https://doi.org/10.1038/s41560-022-01098-3>.
- [167] Mogensen MB, Chen M, Frandsen HL, Graves C, Hansen JB, Hansen KV, et al. Reversible solid-oxide cells for clean and sustainable energy. *Clean Energy* 2019; 3:175–201. <https://doi.org/10.1093/ce/zkz023>.